Information Processing Strategies and Pathways in the Primate Visual System·

David C. Van Essen
and
Charles H. Anderson
Department of Anatomy & Neurobiology
Washington University School of Medicine
St. Louis, MO

INTRODUCTION

The mammalian visual pathway is an amazingly complex and intricate system, capable of processing vast amounts of sensory information for use in the precise control of both immediate and long-term behavior. In many respects, the system is very well engineered for efficient extraction and encoding of information. To give just one example, it is well known that the spacing between photoreceptors in the region of highest acuity is closely matched to the limits of resolution imposed by the physical optics of the eye (Snyder & Miller, 1977). In this chapter, we consider how the notion of "good engineering" can help to understand information processing strategies used throughout the visual system. While some aspects of human vision are mentioned, our analysis will focus on the macaque monkey, which has a superb visual system very similar to that of humans.

Our analysis starts in the retina, where there is a highly selective pruning of the information that enters the eye. In addition, a number of sophisticated data compression schemes are introduced to obtain efficient utilization of the information-carrying capacities of the optic nerve. It is important to understand the representations that emerge from these operations, because they impose major constraints on what can occur at subsequent stages of analysis in the visual cortex.

Several major pathways, including the "parvocellular" and "magnocellular" streams, originate within the retina and diversify within the cortex, producing a rich set of data pathways interconnecting a multitude of higher visual areas. The organization of visual cortex will be discussed at the coarse-grained level of large neural ensembles (areas, layers, and compartments) and also at the fine-grained level of individual neurons and local network architecture. Where possible, systems and computational issues that relate to neuronal architecture will be considered. If evolutionary pressures have driven the entire system towards some near-optimal configuration, the properties of individual components should be related to system performance as a whole.

This chapter also emphasizes the need for dynamic control of the flow and form of information in the brain, an aspect of neural systems that is often overlooked. In general, our perceptions of the world are not derived from isolated, instantaneous glances. Rather, our eyes are in constant motion, moving between selected points of interest. Internal representations of the world are built up over the course of many of these saccades and are continuously updated as the external world changes. An analogous process takes place within the brain in the form of selective visual attention, where detailed scrutiny is applied only to objects within a restricted, but dynamically changing, portion of the visual

· In: An Introduction to Neural and Electronic Networks, 2nd ed., 1995, Academic Press, Zornetzer et al., eds., pp. 45-76

field (Julesz, 1984; Posner & Presti, 1987; Van Essen, Olshausen, Anderson, & Gallant, 1991). These and other observations (cf. Baron, 1987; Kosslyn, 1988) suggest that brain function involves a set of dynamically controlled and hierarchically organized processes. Knowledge of the structure of the visual areas of the cortex provides clues as to where and how this selective control might take place.

THE RETINO-GENICULATE PATHWAY

Overview

The basic layout of the first three stages of the visual pathway in the macaque monkey is illustrated in Figure 1. Each visual center (retina, lateral geniculate nucleus, and primary visual cortex) is a convoluted and/or curved sheet of tissue; they are shown here as flattened, two-dimensional representations that preserves the relative area of each structure. Light from the three-dimensional world is focused by the cornea and lens to form a two-dimensional image on each retina. This image is convened to electrical signals by a dense array of photoreceptors along the back surface of the retina. The number of cones, used for diurnal vision, is about 3 x 10^6 in the macaque and 6 x 10^6 in humans; the number of rods, used for nocturnal vision, is about 10^8 (Østerberg, 1935; Perry & Cowey, 1985).

After processing within several intermediate layers of the retina, information converges onto a population of one million retinal ganglion cells, which comprise several anatomically and physiologically distinct classes of output cell. About 90% of all ganglion cells project to the lateral geniculate nucleus (LGN), somewhat fewer than half going to the same side of the brain and somewhat more than half going to the opposite side (Perry, Oehler, & Cowey, 1984; Fukuda, Sawai, Watanabe, Wakakuwa, & Morigiwa,, 1989). Individual LGN cells relay the outputs of retinal ganglion cells in approximately 1:1 fashion to the striate cortex (area V1). At the cortical stage there is a vast expansion in the neural machinery available to process these inputs, amounting to hundreds of cortical neurons for each LGN input (Schein & De Monasterio, 1987).

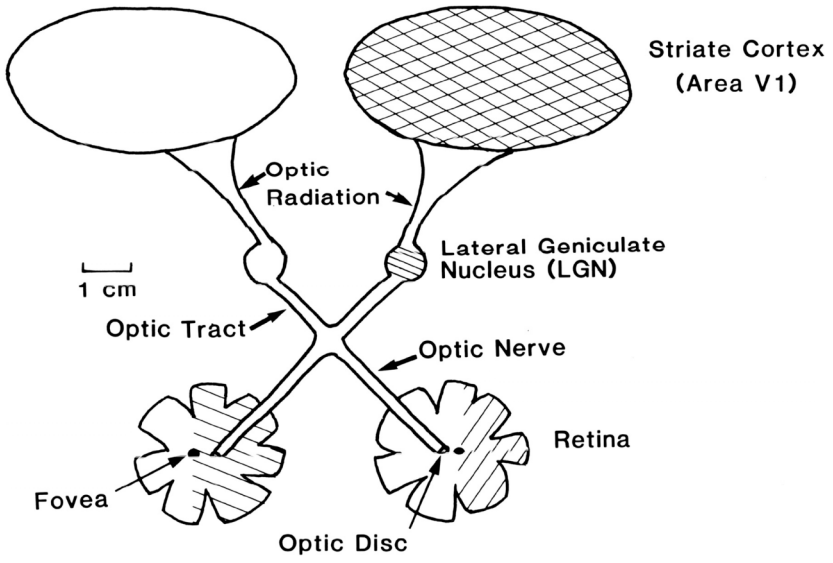

FIGURE 1 A schematic diagram of the retino-geniculo-striate pathway in the macaque monkey. Each visual center is shown as it appears after unfolding and flattening, with preservation of relative sizes. Each retina is about 600 mm^2 in surface area. Since they are hemispherical structures, cuts along the margin are made in order to flatten them. The LGN is a layered structure about 2 mm thick, and in surface area it is less than one-tenth the size of the retina (ca. 45 mm^2 for the outermost layer). The striate cortex (V1) is twice the size of the retina (1200 mm^2 in area in each hemisphere) and is about 2 mm thick. The right hemisphere receives inputs from both eyes, but only from those regions (hatched) subserving the left half of the visual field: about 60% of the left (contralateral) retina and 40% of the right ipsilateral) retina. In the LGN, inputs from the two eyes are segregated into three pairs of layers, with the topmost subserving the contralateral eye. In the cortex the left and right eye inputs initially remain segregated into ocular dominance stripes within layer 4 before intermixing occurs in the superficial and deep layers.

A Scale lnvariant Sampling Strategy

In a standard CCD electronic camera, images are focused onto a uniform, rectangular array of nonoverlapping detectors (pixels). The resolution at which fine details can be analyzed is limited by the degree of blurring of the image and by the spacing of pixels in the array. Ideally, pixel spacing and image blur should be matched to one another. Sampling

too coarsely can cause aliasing, that is, ambiguities in interpretation that can arise when an image is sampled more sparsely than prescribed by the Nyquist sampling theorem. Finer sampling tends to be wasteful, since it would exceed the optical resolution of the camera.

It is important to consider similar issues of image sampling in biological vision, even though the retina differs in many ways from an electronic camera. A particularly striking difference is that the primate retina is a variable resolution system, with extremely high acuity in the fovea and vastly poorer acuity in the periphery. In between these extremes, psychophysical data show an approximately linear change in resolution as a function of eccentricity in the visual field, that is, angular distance from the center of gaze (Westheimer, 1979). The linear nature of this relationship has interesting implications with regard to how much information the visual system transmits about objects in the visual field and how this depends on the distance from which the objects are viewed.

To illustrate this point, it is useful to consider the *sampling lattice* shown in Figure 2, which has a linear fall-off in resolution. After discussing the nature of this representation in the abstract, we will consider its relationship to the sampling strategy used by the retina, particularly at the level of retinal ganglion cells. The lattice contains an array of *sampling nodes,* indicated by dots in the figure. As noted by Koenderink and van Doorn (1978) this pattern has the appearance of a sunflower heart. The basic lattice can be described by two variables. One is the *sampling interval,* corresponding to the distance between adjacent nodes, which increases linearly with distance from the center. (There is some local scatter superimposed, which also occurs in the retina.) The second variable is the sampling area, corresponding to the domain over which information is integrated at a given node. We presume that the sampling area has a Gaussian sensitivity profile, with a width at half height indicated by the circles around some of the sampling nodes in the figure. By having these two variables scale together, all points on the retina are covered, and the degree of overlap between adjacent sampling areas is similar across the whole lattice.

Sampling with a linear decline in resolution (i.e., a linear increase in the sampling interval) leads to the property of scale invariance (van Doorn, Koenderink, & Bouman, 1972). In such a representation the amount of information about any particular object in the visual field remains roughly constant as it is moved closer or further away from the observer, except for gain or loss of information near the center of the image. Consider as a specific example the outline of a hand that is projected onto the sampling lattice in Figure 2. (Imagine, for the moment, that this represents a sampling lattice for your retina and that you are fixating the palm of your outstretched hand.) When the hand is distant, it forms the smaller of two images on the lattice. When the hand is moved closer, cutting the distance in half, the image is enlarged by a factor of two; its margins are a factor of two farther into the periphery; and it is sampled at half the resolution. For instance, in both images there are three or four sampling nodes spanning the tip of each digit. Hence, the amount of information transmitted about the shape of the hand is roughly the same at both scales. Obviously, there is more information about the texture of the center of the palm when the hand is closer. However. changing the distance alters the information content mainly in the region subserved by the center of gaze (or in the extreme periphery if the object becomes larger than the field of view). This analysis applies only when fixating a point near the center of the object, but that is indeed the case much of the time during normal visual behavior.

For a completely scale-invariant system, the sampling interval would decrease literally to zero at the center of gaze. This is clearly impossible for biological vision. because there is a finite limit to resolution and a corresponding minimum size for photoreceptors. The compromise arrangement worked out by nature involves a sampling interval *(D)* that starts at a minimum value (δ) at the center of gaze and increases linearly with eccentricity with a slope (α):

$$D = \delta + \alpha E = \alpha(E_o + E) \approx 0.01(1.3 + E) \text{ deg} \quad (1)$$

The estimated values for the primate visual system ($\delta \approx 0.01°$, $\alpha \approx 0.01$) are based on human psychophysical data and on anatomical data from the macaque retina. The coarseness of sampling in the far periphery (60°) is illustrated on the right of Figure 2, where the spacing is about 50-fold greater than in the center of the fovea; this corresponds to a 2,000-fold difference in the areal density of sampling nodes.

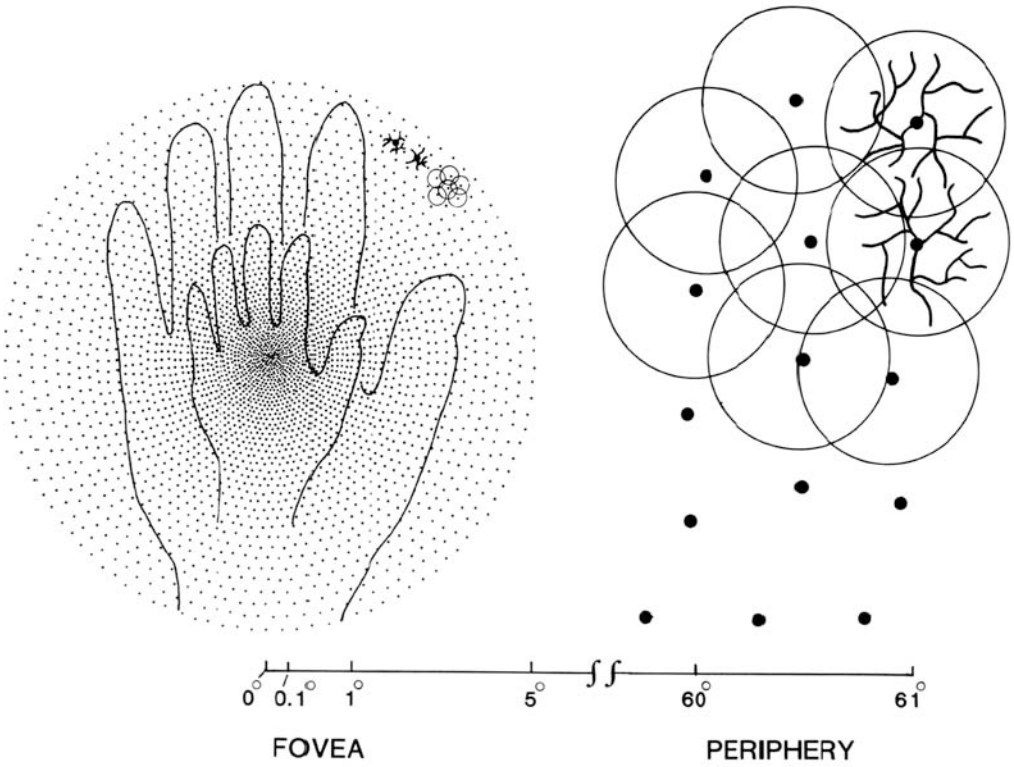

FIGURE 2 A scale-invariant sampling strategy similar to that represented at the level of retinal ganglion cells. On the left is a lattice in which the sampling interval between adjacent nodes increases linearly with distance from the center. The equation used to generate the lattice is $D = 0.06 (E + 0.9 E_{max})$, where E_{max} is the eccentricity at the perimeter of the lattice. In order to provide a visually distinct gradient, the slope for the equation was set much higher than that found in the primate retina (cf. Figures 3 and 4). Nonetheless, with the aid of the nonlinear scale shown at the bottom, the figure also conveys a quantitative indication of the retinal sampling density at different eccentricities. In the far periphery (60° eccentricity), the sampling interval (0.5°) is almost 50-fold lower than at the center of the fovea, as indicated on the right. The number of sampling nodes along a circumferential ring increases gradually with eccentricity, reaching an asymptotic value of $2\pi/\alpha$; this number is 105 for the example illustrated, but is 600-800 for the primate retina. Each sampling node conveys information about illumination in a small region, the sampling area. In a well designed system each sampling area should have a smooth sensitivity profile, the width of which scales with the sampling interval, as indicated by the circles around a few nodes. A few nodes also have a neuron with a dendritic field drawn in, to illustrate how neuronal geometry can be related to the sampling area. In the retina, more than one neuron is typically available to transmit information from each sampling node.

Using this strategy, the entire visual field can be represented with about 300,000 samples, which is comparable to the total number in a CCD camera having a 500 x 500 uniform sample array. To achieve a resolution of 0.01° uniformly over the whole field of view would require hundreds of times as many samples. This is by far the most important data reduction step taken by the visual system. Over 99% of the information available to the photoreceptors is discarded very early on. With inhomogeneous sampling, the entire field is available at varying degrees of resolution; detailed scrutiny of particular regions can be obtained by appropriate eye movements.

Retinal Sampling Strategies

The neural basis for scale-invariant sampling lies mainly within the retina. It reflects how image data are acquired by the cones and how they are further processed and encoded by the ganglion cells. It is particularly important to assess the issue at the ganglion cell level, because the optic nerve is a critical bottleneck through which all visual information must flow. Acuity and other aspects of vision are fundamentally constrained by the information represented at the level of retinal ganglion cells (cf. Rovamo & Virsu, 1979). However, it is also important to understand the nature of the initial neural representation provided by the cones.

Each node in a sampling lattice conveys information about what is happening in a small patch of the retina. In principle, this could be mediated by a single channel, as is suggested by the inclusion of only one neuron per sampling node in Figure 2. However, it is entirely reasonable to have more than one channel per node, especially because there are several types of information to be conveyed (e.g., distinctions of color and light versus dark features). In addition, real neurons operate using a limited range of firing rates, and more data can be conveyed by increasing the number of output neurons at each node. This multiple-neuron strategy does indeed appear to be used, and it leads to the notion of a sampling multiplicity (coverage factor) to signify the number of neural channels per sampling node. Another important factor is that there are two major ganglion classes that operate at different spatial scales. Hence, it is necessary to think in terms of two distinct sampling lattices within the retina that work together for the efficient encoding of spatial and temporal information.

Photoreceptor Distribution

Cone spacing and size increase relatively rapidly within the fovea (central 2°), but much more slowly at higher eccentricities (Figure 3, solid line). There is a progressive mismatch between cone spacing and the sampling interval for the main class of ganglion cell (dashed line). This signifies that the number of cones within each sampling area increases with eccentricity, approaching 20-30 cones per node in the periphery (Wässle & Boycott, 1991).

The center of the fovea is occupied exclusively by long-wavelength (L) and medium-wavelength (M) cones, whose broad absorption spectra are only slightly displaced from one another. Short-wavelength (S) cones, whose absorption spectrum is more substantially displaced toward short wavelengths, are more sparsely distributed. At their peak they represent only about 7% of the cone population (De Monasterio, McCrane, Newlander, & Schein, 1985).

Rods, which have the high sensitivity needed for nocturnal vision, are absent in the center of the fovea but rapidly increase in density outside the fovea, thereby providing a high collection efficiency for all but the central few degrees. In the periphery, rods are densely packed and cones are relatively sparsely spaced. Interestingly, the spacing between cones changes more rapidly than the decline in optical quality of the image in the periphery. Hence, peripheral images are spatially undersampled, and some aliasing can occur in principle. However, this aliasing is unlikely to introduce a significant contamination of the information represented at the ganglion cell level, because ganglion cells in the periphery integrate inputs from many cones and transmit only low resolution data (Williams & Collier, 1983).

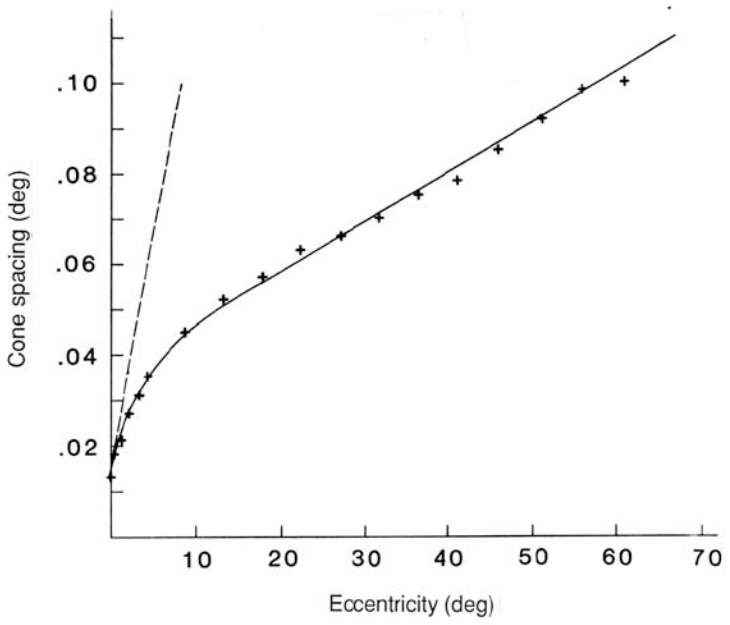

FIGURE 3 Cone spacing in the macaque retina. Values are calculated assuming hexagonal packing of cones and using published data on cone densities (Perry & Cowey, 1985). Numerical data was kindly provided by H. Perry. Only values for dorsal, ventral, and temporal retina are included because of the systematically higher cone density in the nasal quadrant. At the center of the fovea, cone spacing is about 0.013° (ca. 3 □m). The initial part of the curve is fit by the equation $D = 0.01(E + 1.3)^{\circ}$, which provides one estimate for the canonical sampling lattice in the retina (dashed line). At higher eccentricities, cone spacing continues to increase. but much more slowly than the canonical sampling interval. Other estimates for how the sampling interval changes with eccentricity in macaques and humans generally show a slope (α) ranging from 0.007 to 0.01 and an *x*-intercept (Eo) between 0.8° and 2.5°; these are based on data for cone spacing (De Monasterio, McCrane, Newlander, & Schein, 1985; Williams, 1988), ganglion cell density (see Figure 4), and visual acuity (cf. Westheimer, 1979). The *x*-intercept ($E_0 = 1.3^{\circ}$) indicates where the system makes the transition from scale invariance (E>>Eo) to translational invariance (E<<Eo). Thus. vision is largely scale invariant outside the fovea (central 2°), largely translation invariant in the central 0.5°, and smoothly graded in the intermediate region.

Retinal Neural Layers

The highly stereotyped architecture of the retina includes only five major neuronal types. The most direct route for information flow is from photoreceptors to bipolar cells and from there to ganglion cells. Horizontal cells provide an alternate route from photoreceptors to bipolar cells, as well as feedback to photoreceptors. Amacrine cells mediate interactions in both directions between bipolar cells and ganglion cells. This complex network implements a variety of data compression schemes aimed at emphasizing information that is "useful" (behaviorally salient) at the expense of data that is relatively unimportant or can be transmitted with lower fidelity (cf. Laughlin, 1987; Atick & Redlich, 1992)

The specific strategies described next reflect three important characteristics of information processing in the visual system. One is an emphasis on data compression techniques such as differentiation in the domains of space, time, and spectral composition, which is done in order to reduce redundancy in the signals transmitted by neighboring neurons (cf. Adelson & Bergen, 1991). The second is division of labor by creation of multiple cell types. The third involves multiplexing of information so that each cell, while functionally specialized, is nonetheless able to carry more than one type of information. Our focus here is on the general nature of these strategies; useful reviews and references pertaining to the detailed neural circuitry are provided by Dowling (1987), Rodieck (1988), and Wässle & Boycott (1991).

Spatial Differentiation Both bipolar cells and ganglion cells have receptive fields with a characteristic center-surround organization, in which the direct input from one or more cones is counterbalanced by antagonistic inputs from a wider region that is generally presumed to be mediated by neighboring horizontal cells (but see Reid and Shapley, 1992). This spatial differentiation emphasizes local differences in light intensity at the expense of precise information about absolute intensities.

On and Off Channels All photoreceptors respond with a graded hyperpolarization (more negative membrane potential) to an increase in light intensity. In contrast. at the bipolar cell stage only half the cells are hyperpolarized by light onset in the receptive field center ("off" bipolars); the other half are depolarized by light onset ("on" bipolars). This dichotomy between on and off channels is preserved at the ganglion cell stage and beyond. This is advantageous because ganglion cells convey information using a firing frequency that is modulated around a low to moderate level of spontaneous activity. Ganglion cells and, to an even greater degree, their targets in the LGN act as rectifiers. Since dark stimuli on a light background (e.g., the print in this book) are just as important as light stimuli on a dark background, the dual-channel arrangement of ganglion cells provides a conveniently balanced, symmetrical output representation.

Parvocellular and Magnocellular Channels Superimposed on the on/off dichotomy is another classification scheme that is based on cell size, projection patterns, and the type of information encoded by ganglion cells (Perry et al., 1984; Shapley & Perry, 1986). The vast majority of ganglion cells (about 80%) have relatively small cell bodies, axons, and dendritic arbors; they are commonly called parvocellular (P) cells. Cells in another important class, commonly called magnocellular (M) cells, have larger cell bodies, axons, and dendritic arbors. Both P and M cells project to the LGN; the remaining 10% of ganglion cells comprise a heterogeneous group with small axons, some of which probably project to the LGN (Conley & Fitzpatrick, 1989) and others to the superior colliculus (Perry & Cowey, 1984).

Temporal Differentiation Time-dependent changes in illumination at a single retinal location can be as meaningful as spatial differences in illumination, so it is not surprising that temporal differentiation is an important aspect of retinal processing. There are striking differences in temporal processing between P and M cells (Marrocco, McClurkin, & Young, 1982; Hicks, Lee, & Vidyasagar, 1983; Crook, Lange-Malecki, Lee, and Valberg, 1988). P cells tend to give sustained responses to a maintained stimulus; they typically respond best to patterns modulated at around 10 Hz; and they often cannot follow modulations more rapid than 20-30 Hz. M cells, in contrast, respond only transiently to a maintained stimulus; they usually respond best to modulation at 20 Hz or greater; and they continue to respond up to

60-80 Hz. Amacrine cells are suspected to be the major source of this temporal differentiation by the magnocellular pathway. Some M cells also respond to abrupt motion of patterns well outside the classical receptive field, indicating a more complex type of spatio-temporal processing (Kruger, 1977; Marrocco et al., 1982).

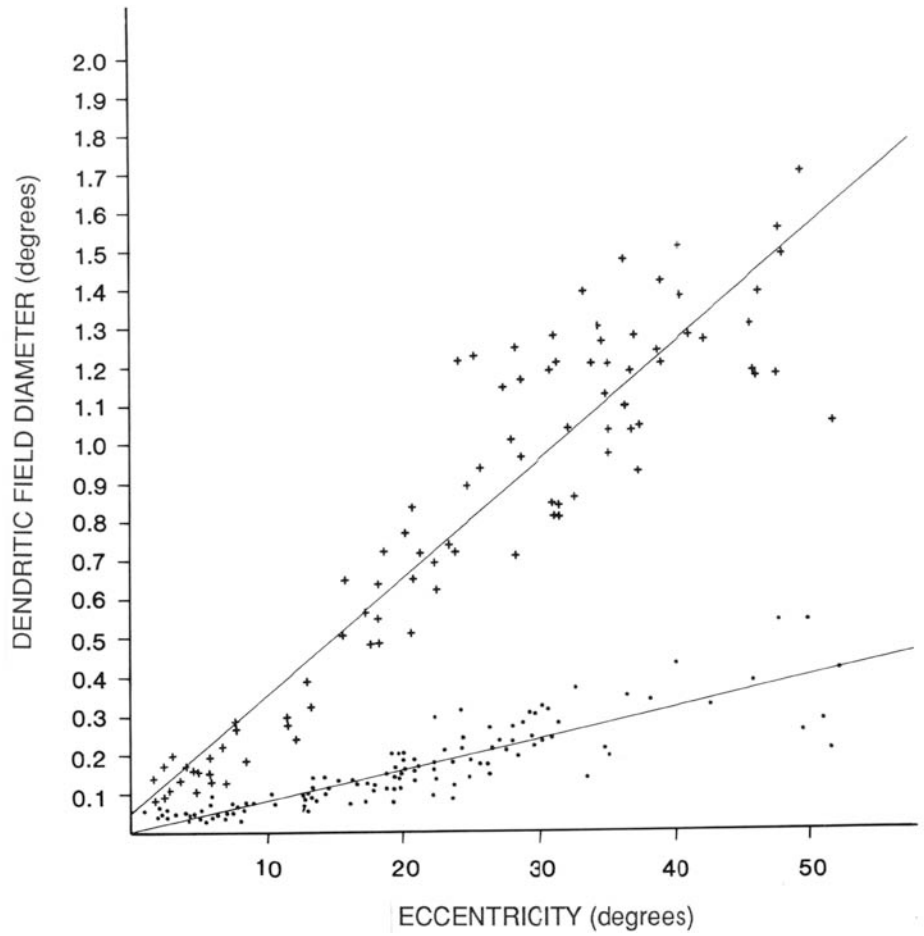

FIGURE 4 Dendritic field diameters of P and M ganglion cells in the macaque retina (based on Perry, Oehler, & Cowey, 1984). Outside the fovea, ganglion cells are more densely packed in the nasal retina than at the equivalent eccentricity in the temporal retina, and they have correspond-ingly smaller dendritic field arbors. In order to compensate for this systematic bias. we shifted the data points for nasal ganglion cells to eccentricities that were slightly closer to the fovea (34% closer for ganglion cells on the horizontal meridian and 23% closer for cells on the nasal side but away from the horizontal meridian). This adjustment was based on the magnitude of the reported ganglion cell density differences, and it noticeably improved the correspondence between dendritic diameter and eccentricity relative to their published results. The P cell data (dots) are fit by the regression line $D = 0.008 (E + 0.03)^{\circ}$; the M cell data (crosses) by $D = 0.03 (E + 1.7)^{\circ}$. Near the fovea the data points are unreliable because there is substantial offset between ganglion cell bodies and the cones to which they are linked, and also because the P cell dendritic size reaches a minimum that reflects the size of cone cell synaptic terminals (Schein, 1988).

Spectral Differentiation P cells carry chromatic information by virtue of the spectral opponency of their receptive fields (De Monasterio, 1978; DeVaolis & DeValois, 1993; Reid & Shapley, 1992). As might be expected from the relative numbers of cone types, most P cells have red-green opponency, but a small minority have blue-yellow opponency. M cells are not overtly spectrally opponent, but they can respond in a nonlinear fashion to the presence of spectral contrast (Lee, Martin & Valberg, 1989).

Sampling Multiplicity of P and M Cells

The sampling multiplicity, or retinal coverage factor, provides a measure of how many ganglion cell receptive fields of a given class overlap one another at each point on the retina (Peichl & Wässle, 1979). Anatomical data on dendritic field sizes of P and M cells (Perry et al., 1984; Watanabe & Rodieck, 1989) can be used to estimate how the sampling area varies with eccentricity. For both populations, dendritic field size increases linearly with eccentricity, but the slope is three-fold greater for M than for P cells (Figure 4). The physiologically determined size of receptive field centers is also substantially greater for M cells than P cells (DeMonasterio and Gouras, 1975; Derrington and Lennie, 1984). Some studies have emphasized that P and M cells have similar high-frequency cutoffs when acuity is measured using high-contrast gratings (Hicks et al., 1983; Blakemore and Vital-Durand, 1986; Crook et al., 1988). However, grating acuity is an unreliable measure of receptive field center size (see below and legend to Fig. 5).

These findings, in conjunction with data on ganglion cell densities (Wässle, Grünert, Rohrenbeck, and Boycott, 1990) indicate that there are about 3-5 P cells per sampling area in the periphery, which allows for separate handling of

information from the different chromatic channels as well as the "on"' and "off"' attributes. Earlier studies (Van Essen & Anderson, 1986; Schein 1988; Perry & Cowey, 1985; 1988) estimated the coverage factor in the center of the fovea to be two or less, where single L or M cones presumably drive the center receptive field of "on" and "off" P cells. Wässle et al. (1990), working with single retinas to eliminate uncertainties introduced by individual variation, found a notably higher value of 3-4 ganglion cells per cone in the center of the fovea. This suggests that the P cell sampling multiplicity may be roughly constant throughout the retina.

A similar analysis can be applied to the M cell sampling mosaic. The incidence of M cells (as a percentage of all ganglion cells) is 5% - 6% in the fovea and parafovea (Grünert, Greferath, Boycott, and Wässle, 1993) and increases to 10% - 12% over most of the retina (Perry et al., 1984), and about 20% in the far periphery (Silveira and Perry, 1991). The ratio of M/P dendritic field sizes is about 3 over a wide range of eccentricities (see above; Fig. 4), but inside 10° the ratio increases to about 5 in the macaque (Watanabe and Rodieck, 1989) and even higher in the human (Dacey and Petersen, 1992). The decreased incidence and increased relative size tend to cancel out, and as a result the estimated sampling multiplicity for M cells is approximately constant at about 3 - 4 over a wide range of eccentricities (Perry and Cowey, 1985; Grünert et al., 1993).

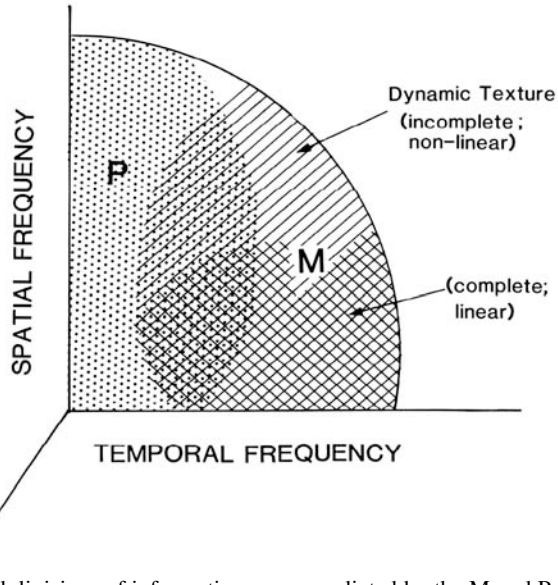

FIGURE 5 Subdivisions of information space mediated by the M and P subsystems. Each small patch of retina is subserved by a population of cones and bipolar cells whose spatial and temporal bandwidth is represented by the area within the solid outline. Only one dimension of spatial frequency is shown, but the second dimension could be incorporated using the unlabeled axis included in the figures. Individual ganglion cells are only able to represent information across a portion of the entire domain. P cells subserve the domain of low temporal frequencies, including both low and high spatial frequencies (stippled area). M cells subserve mainly higher temporal frequencies, and they also span a wide range of spatial frequencies. At low spatial frequencies responses are largely linear (cross-hatched region) and their high-frequency cutoff is on average only slightly less than that of P cells despite their larger receptive field center size. This may reflect the higher contrast sensitivity of M cells compared to P cells (Purpura, Kaplan & Shapley, 1988) and also the nonlinear properties of some M cells (Derrington & Lennie, 1984), which together should enhance the responses to gratings and textures that are much finer than the receptive field center. In addition, optical blurring (i.e..the point spread function) should affect the high-frequency cutoff of P cells more than M cells, because P-cell receptive fields are more closely matched to the optical limits of the retina. Responsiveness in the single-hatched region can signal the presence of dynamic texture (fine-grained, rapidly changing patterns in an image). However, complete fidelity in a representation of this region would necessitate as many M cells as P cells. Since M axons are thicker than P axons, this would more than double the diameter of the optic nerve, which in turn might impair ocular mobility.

Functional Division of Labor in the Retina

The differences between P and M cells represent a systematic division of labor in transmitting spatial, temporal, and chromatic information to the cortex. We believe that this reflects a strategy for packing the maximum amount of useful information into the optic nerve, given the finite transmission rates and finite diameters of real axons (Wolbarsht, Wagner, & Ringo, 1985; Anderson, 1986).

A convenient way of summarizing this strategy is illustrated in Figure 5. The region of information space associated with a small patch of retina can be conveniently represented in a two-dimensional plot showing temporal frequency along the *x* axis and one dimension of spatial frequency along the *y* axis. The solid line outlines the portion of this space from which information can in principle be transmitted, given the spatial constraints that are imposed by the retinal sampling lattices for cones and ganglion cells and the temporal constraints that are imposed by the firing rates, integrative properties, and intrinsic physiological noise of retinal neurons. Within this overall domain, P cells (stippling) and M cells (hatching) subserve partially overlapping, but substantially distinct regions as a result of their different temporal properties. P cells handle low temporal frequencies, M cells handle high temporal frequencies, and both types overlap considerably in the region of intermediate frequencies.

In the spatial domain, P cells act as relatively linear filters whose wide spatial bandwidth reflects a combination of small receptive field size and incomplete center-surround antagonism. The small size of receptive field centers ensures responsiveness to high spatial frequencies, while the incomplete balance between center and surround mechanisms results in some responsiveness even to very low spatial frequencies (Derrington & Lennie, 1984).

The situation for M cells is more complex. M cells provide a faithful representation of low spatial frequencies at high temporal frequencies, corresponding to coarse, rapidly changing patterns (Figure 5, double hatching, lower right). In addition, M cells respond to high spatial frequencies (Baltimore & Vital-Durand, 1986; Crook et al., 1988), but the representation of dynamic texture in this region is incomplete and of lower fidelity (single hatching, upper right). This is attributable to the nonlinear nature of responses in many M cells (De Monasterio, 1978; Derrington & Lennie, 1984) and also to the fact that the overall number of M cells is insufficient for a complete, unambiguous representation at high resolution (Wässle and Boycott, 1991; Grünert et al., 1993). In short, M cells are able to signal the presence of moving or changing patterns over a wide range of spatial scales and temporal frequencies that can be used to signal the presence of interesting features, but leaves the details to be carried by the P cells.

In the spectral domain, the main points to emphasize are that P cells carry most of the color information about an image, yet this is only a small percentage of the overall information relayed by P cells (cf. DeValois & DeValois, 1992). Psychophysical studies (Noorlander & Koenderink, 1983; Mullen, 1985) have shown that, at all eccentricities, acuity for isoluminant gratings (which differ only in color) is 5-fold to 10-fold worse than for luminance gratings (which differ only in brightness). By this measure the chromatic information in a region of visual space may be as little as 1% ($1/10^2$) of the luminance information. This accounts for the ease with which color television signals have been made compatible with existing black and white standards, since relatively little additional information is required to match our capacity for perceiving color variations within an image (Buchsbaum, 1987).

Lateral Geniculate Nucleus

The LGN contains six main layers, which serve to segregate the inputs from P and M channels and to align the inputs from the two eyes while nonetheless keeping them physically segregated. The upper four layers (parvocellular or P) receive inputs from retinal P cells, while the lower two (magnocellular or M) receive inputs from retinal M cells. There is an approximately 1:1 coupling between ganglion cells and LGN relay cells (Lee, Virsu, & Creutzfeldt, 1983). There is also massive feedback to the LGN from a substantial fraction of the 10 million cells in layer 6 of striate cortex, as well as various sources of nonvisual inputs. The functional significance of this feedback and of the various other inputs to the LGN has not been firmly established, although it is presumably somehow involved in the dynamic regulation of signal transmission (cf. Sherman & Koch, 1986; Casagrande & Norton, 1991). Interestingly, the rates of spontaneous activity and of visually evoked activity are generally much lower for LGN cells than for retinal ganglion cells (Kaplan, Purpura, & Shapley, 1987). An attractive hypothesis to account for this difference is that cortical feedback might suppress transmission in regions where the image is relatively smooth and featureless, while enhancing transmission for regions rich in features. A similar process, called dynamic coring, is used in some television receivers to selectively reduce noise levels in featureless regions of the image. The idea of differential suppression of LGN transmission has also been proposed by Crick (1984) and by Koch (1987) as a mechanism for directed visual attention. We suspect that visual attention instead involves dynamic mechanisms, operating mainly at the cortical level, and that the role of modulatory processes in the LGN is linked to basic signal-to-noise issues rather than attention *per se*.

Summary

The retina samples images in a spatially inhomogeneous fashion that involves a simple linear change in resolution with eccentricity. Luminance information at each sampling locus is compressed using spatial and temporal differencing.

This information is distributed into the parvocellular and magnocellular systems, each with its own "on" and "off" subsystems. The P system handles low to moderate temporal frequencies and carries luminance information from the lowest resolution up to the highest allowed at a given eccentricity. The M system emphasizes luminance at lower spatial resolution, but higher temporal rates. Spectral information is multiplexed into the P system, but constitutes only a small percentage of the total amount of information that it normally carries. Multiplexed into the M system is a nonlinear measure of spatial and/or spectral energy which may be especially useful for texture analysis, image segmentation, and preattentive visual processing.

VISUAL CORTEX AND NEURAL REPRESENTATIONS IN AREA V1

Overall Layout of Visual Areas

The cerebral cortex is the dominant structure of the mammalian brain and the principal site of higher levels of visual processing. The cortex is a thin, laminated sheet of tissue in which the various cortical layers differ in cell density, connectivity, and many other characteristics. As will become apparent, laminar organization is fundamental to understanding cortical function. In the macaque, the total cortical surface area (counting both hemispheres) is about 210 cm^2, equivalent to a large cookie (Felleman & Van Essen, 1991). Given a thickness of 1-2 mm and an average cell density of 10^5 cells/mm^2, this works out to a total population of approximately 2 x 10^9 neurons. More than half of the cortex is related to vision; area V1 (striate cortex or primary visual cortex) alone is about 12% of the total. For comparison, cerebral cortex in the human is about 10 times larger in both surface area and total number of neurons (Blinkov & Glezer, 1968). Area V1 is only twice as large in the human as in the monkey, though, and it occupies only about 3% of the total cortical expanse.

In the macaque, visually responsive cortex occupies all of the occipital lobe, about half of the temporal and parietal lobes, and a small portion of the frontal lobe. This large domain is divisible into many discrete visual areas that can be distinguished from one another on the basis of their overall pattern of inputs and outputs (connectivity). In addition, some areas can also be recognized by other criteria, including cortical architecture (structural appearance after appropriate staining), visual topography (a partial or complete representation of the visual field), and receptive field properties (e.g., selectivity for particular stimulus properties). Altogether, there are 32 identified areas that are largely or exclusively visual, including 7 areas that are associated with visuomotor control, polysensory processing, and/or attentional and cognitive processing (Felleman & Van Essen, 1991). Figure 6 shows the location and relative size of various areas, as displayed on a two-dimensional unfolded map of the cortex. All the boundaries between areas are drawn in, but for simplicity and clarity we have included only the names of the particular areas that are discussed in the following sections. These include areas V1, V2, V3, V4, the middle temporal area (MT), a cluster of six areas in the temporal lobe known collectively as the inferotemporal (IT) complex, and a cluster of areas in the parietal lobe known as the posterior parietal complex (PP).

Broadly speaking, visual information that enters V1 is processed in a highly localized fashion to generate a multitude of data representations for distribution to other areas subserving more specialized analyses (Hubel & Wiesel, 1977; Zeki, 1978). A useful distinction (but one to be made with caution) is that inferotemporal cortex is mainly concerned with object identification, pattern recognition, and aspects of "what" is in the visual world, whereas posterior parietal cortex is concerned with spatial relationships and the assessment of "where" things are (Ungerleider & Mishkin, 1982; Maunsell & Merigan, 1993).

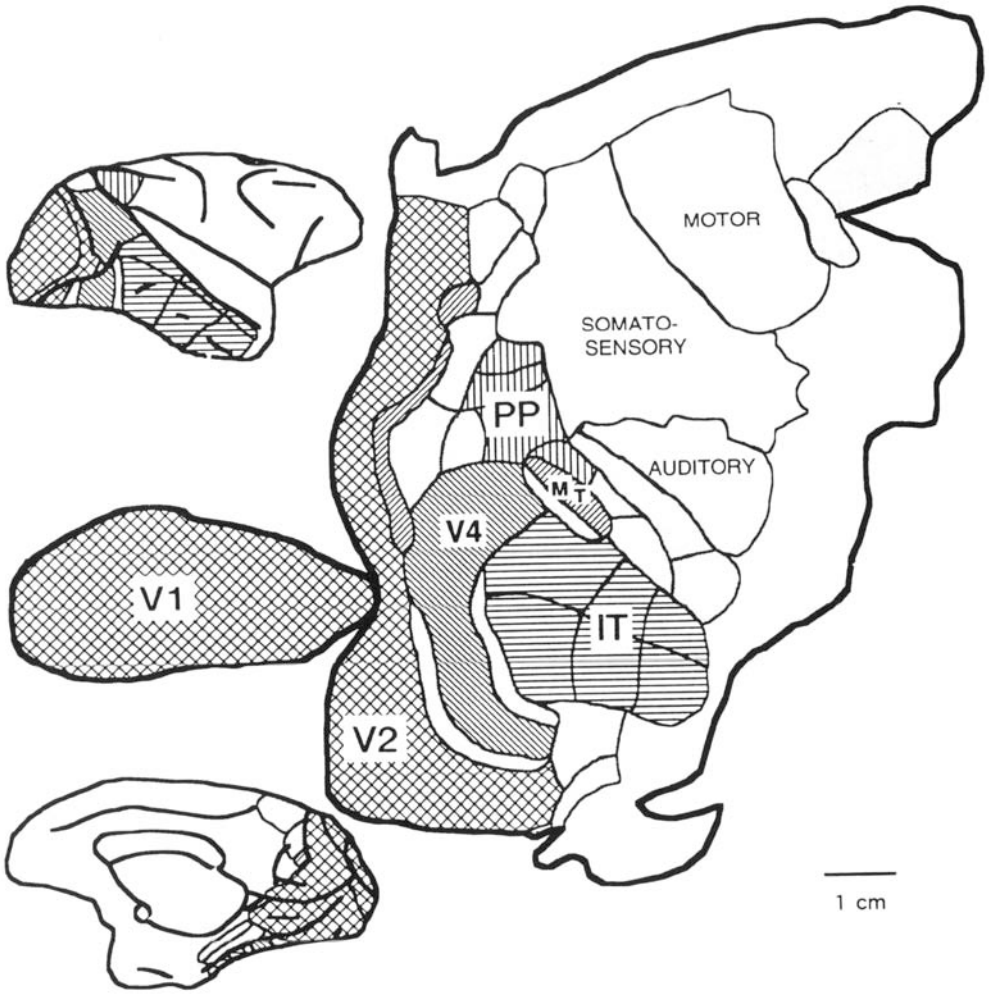

FIGURE 6 Visual areas in the cerebral cortex of the macaque, as seen in lateral and medial views of the right hemisphere *(insets)* and in an unfolded two-dimensional map. Visual cortex occupies more than half of the entire cortex, mainly in the occipital, temporal, and parietal lobes (bold outline on the left on the map), but also in a portion of the frontal lobe. The major visual areas discussed in this chapter are shown by stippling. These include areas V1 (separated from the rest of the map by an artificial discontinuity, but physically contiguous in the intact hemisphere), V2, V4, the middle temporal area (MT), the posterior parietal complex (PP), and the inferotemporal complex (IT). IT and PP each contain many separate areas (Felleman & Van Essen, 1991). There are 14 additional visually related areas not labeled on the map. Modified, with permission, from Felleman & Van Essen (1991).

Architecture, Connectivity, and the Sampling Lattice in V1

V1 receives a precisely organized array of projections from the LGN, which produces a representation of the visual field on the cortical surface shown on the two-dimensional map of Figure 7. There is a great emphasis on central vision, with nearly half the cortex devoted to the central 5˚. To a first approximation, the amount of cortex devoted to the region between 5˚ and 10˚ eccentricity is similar to that from 10˚ to 20˚ and from 20˚ to 40˚, which is a manifestation of the scale-invariant sampling strategy that originates in the retina.

This issue can be analyzed quantitatively by deriving expressions for the cortical magnification factor (mm^2 of cortex per $degree^2$ of visual field) as a function of eccentricity. Physiological mappings of several hemispheres by Van Essen et al. (1984) yielded the relationship described in Equation 2 for a standard visual cortex:

$$M^2 = 140\ (0.78 + E)^{-2.2}\ mm^2\ /deg2 \qquad (2)$$

This equation predicts a ratio of ~4,000 in areal magnification factor for the center of the fovea vs. 60º eccentricity. This is only slightly greater than the ratio of 2,000 predicted from the retinal sampling lattice (Equation 1) or the ratio of 1,000 predicted from the retinal ganglion cell density estimates of Wässle et al. (1990). Even closer agreement is obtained when the retinal data are compared to the results from deoxyglucose mapping experiment of central fields in striate cortex (Tootell et al., 1988). Given that there is substantial individual variability in all of these mappings, it will be necessary to study both retinal and cortical representations in the same individual to obtain a substantially more precise understanding of these relationships.

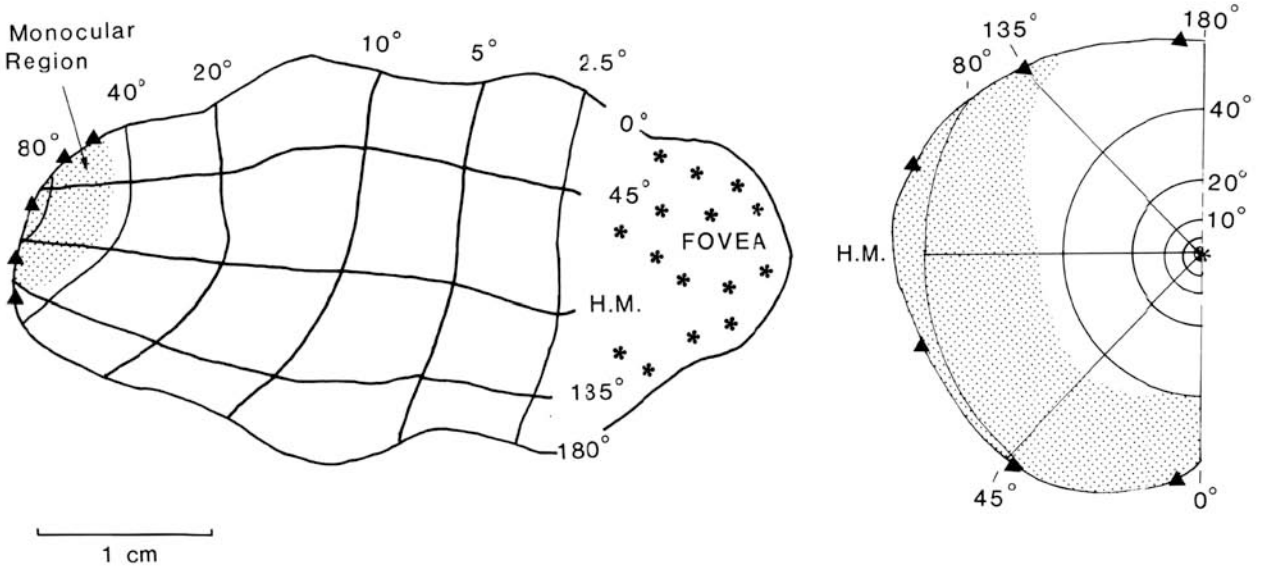

FIGURE 7 Topographic organization of area V1. Lines of constant eccentricity (semicircles in the visual field drawing on the right) map onto contours that run approximately vertically on the cortical map. Lines of constant polar angle (rays emanating from the center of gaze in the visual field) map onto contours that run approximately horizontally on the cortical map; there is also an inversion such that the lower and upper quadrants of the visual field are represented in dorsal and ventral halves of cortex respectively. The foveal representation (asterisks), corresponding to the central 2° radius, occupies slightly more than 10% of V1. Fitting this data to a modified log polar mapping gives a linear cortical magnification factor of $M\alpha\ (0.8+E)^{-1.1}$. We believe this description fits the experimental data and the retinal sampling strategy better than the slightly different log conformal representation suggested by Schwartz (1980). However, there is considerable biological noise in actual cortical topography, both in terms of individual varability in topographic organization and in terms of significant local deviations from the mapping function to make these only approximate mathematical interpolation formulas. (Modified with permission from Van Essen, Newsome & Maunsell, 1984.)

In a standard Nissl stained section, the distribution of cells in Vl is relatively uniform within each layer with no obvious periodicities running parallel to the cortical surface. Lurking beneath this apparent uniformity, however, is a modular organization revealed by several histochemical stains (most notably the enzyme cytochrome oxidase), and also reflected in anatomical connectivity patterns and in the physiological organization of receptive field properties (Hubel & Wiesel, 1974; Livingstone & Hubel, 1984). Most of these patterns have a periodicity on the order of 1 mm. It is therefore of particular interest to ascertain the number and the distribution of cortical cells and of LGN inputs associated with each square millimeter of cortex. The key features of this arrangement are shown in Figure 8, which illustrates the pattern of LGN projections to a 1-mm^2 patch of Vl. P cell inputs are displayed along the front face and the pattern of M cell inputs displayed along the right side.

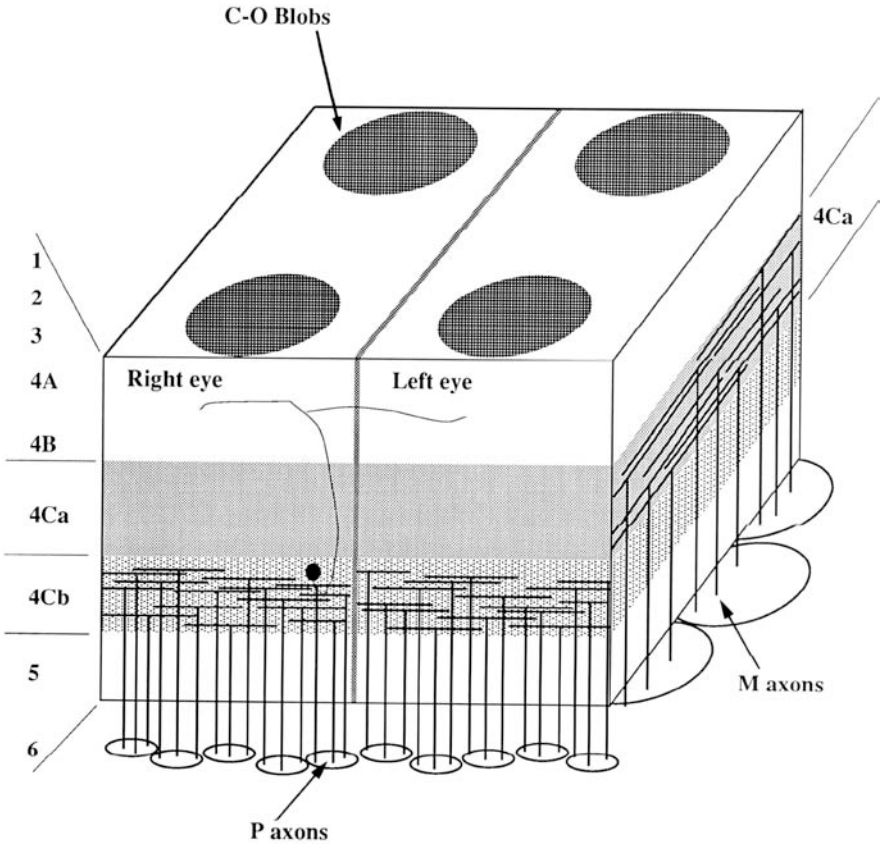

FIGURE 8 Architecture of P and M inputs to area V1. The diagram shows a l-mm^2 patch of V1. with inputs from P cells terminating in layer 4Cb *(front face)* and inputs from M cells terminating in layer 4Ca *(righface)*. Groups of axons associated with a single sampling node are bundled together by the small loops in the white matter. The actual density of P and M inputs and the extent and degree of overlap of axonal arbors within each layer are indicated semi-quantitatively. This figure also shows two manifestations of modular organization within V1: ocular dominance stripes, in which there is sharp segregation of the inputs from left and right eyes in layer 4, and cytochrome oxidase "blobs,-- shown as circular patches on the surface of the cortex that are positioned along the center of each ocular dominance stripe. The spacing of lettering on the left provides a more accurate indication of the relative thickness of different layers than does the actual figure, in which layer 4C has been expanded for clarity.

Each square millimeter of cortex receives on average about 800 P cell afferents (400 per eye) and about 80 M cell afferents (40 per eye). In relation to the P and M sampling lattices outlined previously, each square millimeter is supplied by about 120 sampling nodes from each eye for the P system (represented by loops around sets of P cell inputs) and about 12 sampling nodes from each eye for the M system.

V1 has many more distinct layers than are found in other cortical areas, which stems in large part from the segregation of P and M pathways (Hubel & Wiesel, 1977, Fitzpatrick, Lund, & Blasdel, 1985). P inputs terminate mainly within a thin sheet known as layer 4Cb, whereas M inputs terminate immediately above, in layer 4Ca. In each of these layers there is also a clear segregation of inputs for the two eyes. This is manifested by an alternating series of ocular dominance stripes. each approximately 0.5 mm wide and receiving inputs exclusively from one eye.

The axonal arbors of P cell afferents are relatively compact, with a typical arbor diameter of 150-250, □mg which is reflected in the horizontal extent of axons drawn in the figure (Blasdel & Lund, 1983). Dendritic arbors of cells in layer 4Cb are also about 150-200 μm in diameter (Lund, 1988). Based on these numbers and on the density of P cell afferents, it follows that each cell in layer 4Cb can potentially be in physical contact with about 100 P cells. We estimate that each neuron in layer 4Cb receives about 100 geniculo-cortical synapses, based on the data of O'Kusky and Colonnier (1982) and Blasdel and Lund (1983). Likewise, each cell in layer 4Ca receives a total of about 100

geniculo-cortical synapses from up to 100 M cells, whose axons are much larger but whose innervation density is much lower. However, it is not known how different geniculate axons contribute to the innervation of each cortical cell.

The segregation of M and P pathways is remarkably sharp at subcortical levels and in the geniculocortical afferent terminations. However, within the cortex there is considerable intermixing that begins even within layer 4C by virtue of dendritic and local axonal arbors that cross between layers 4Ca and 4Cb. In the supragranular layers of cortex, there are three major compartments: layer 4B and the cytochrome oxidase (CO) enriched "blobs" and CO-sparse "interblobs" of layers 2 and 3. Layer 4B is dominated by inputs from the M pathway, but the blobs and interblobs each receive major influences from both P and M inputs, (see below).

Physiological Properties in V1

Single unit recordings have revealed that neurons in V1 comprise a diverse and heterogeneous population, in contrast to the more stereotyped nature and limited number of cell classes in the retina and LGN. This is commensurate with the large increase in the number of cells available for processing information from each patch of the visual field. As a population, cells in V1 have more than a dozen important receptive field characteristics representing the emergence of new properties or the refinement of existing properties of LGN cells. Most of these reflect highly local computations that take advantage of the precise topography in the organization of the ascending inputs to V1. However, some properties reflect the operation of feedback pathways and/or long distance lateral interactions.

Orientation and Spatial Frequency Two particularly important and intertwined characteristics are orientation selectivity and spatial frequency tuning. Except in layer 4Cb and the CO blobs, the majority of V1 cells show at least some selectivity for stimulus orientation (often very sharp tuning) and they are much more narrowly tuned for spatial frequency than are their LGN inputs (Hubel & Wiesel, 1968; DeValois, Albrecht, & Thorell, 1982; Blasdel & Fitzpatrick, 1984; Livingstone & Hubel, 1984). In simple cells, whose receptive fields can be subdivided into separate excitatory and inhibitory subregions, the overall profile of sensitivity can be approximated by a Gaussian weighted sine wave (Daugman, 1985; Jones & Palmer, 1987). A population of such cells tuned for an appropriate range of orientations and spatial scales can provide a complete representation of an image down to the limit of spatial resolution. Moreover, this is an efficient form of representation insofar as the outputs of different cells in response to natural images will tend to be statistically independent of one another (Daugman, 1985; Field, 1987; C. H. Anderson, unpublished results).

Another major cell class is the "complex cell", in which orientation selectivity is also present, but the cell is relatively insensitive to the exact position of the stimulus (Hubel & Wiesel, 1962; Pollen, Goska, & Jacobsen, 1988; Jacobsen et al, 1992). This strongly nonlinear property suggests that complex cells signal a spatially averaged energy associated with a particular orientation. This is analogous to the nonlinear behavior of many M cells in the retina and LGN, as discussed already. As with M cells, such an energy measure may be useful for image segmentation and texture analysis.

Velocity Another property involves selectivity for stimulus velocity—the direction and speed of motion. Velocity selectivity can be regarded as a form of spatio-temporal filtering, in which a cell responds optimally to a target moving along a particular orientation in space-time coordinates (Adelson & Bergen, 1985). If the spatio-temporal filter is strictly linear, then the preferred direction should reverse with a change in stimulus contrast (i.e., from dark to light), as has been reported for some cells in layer 4B (Livingstone & Hubel, 1984). Nonlinearities at a subsequent processing stage can yield directional preferences that are contrast independent.

Binocular Interactions Interactions between the two eyes are obviously important for binocular fusion (a single percept emerging from two separate views of the world) and for stereopsis (judgments of depth based on the small binocular disparities arising from the different viewing angles of the two eyes). Cells in layer 4C are monocularly

driven, just like their LGN inputs, but in other layers most cells can be activated through either eye. A substantial fraction of the cells in V1, particularly in layer 4B, show tuning for binocular disparity (Poggio, 1984).

Spectral Composition Most cells in the blobs of V1 are wavelength selective, and many have properties that are more complex than the basic center-surround chromatic opponency characteristic of P cells in the retina and LGN. Also, many cells in the interblobs show wavelength selectivity in addition to orientation selectivity (Livingstone & Hubel, 1984; Michael, 1985; T'so & Gilbert, 1988).

Length and Curvature Many V1 cells have the property of end-stopping, whereby the response to a long bar is much less than that to a short bar (Gilbert, 1977). The activity of these cells may be useful in signaling information about terminations, corners, and even smooth curvature of contours in the visual field (Dobbins, Zucker, & Cynader. 1987). End-stopping could also contribute to the responses to texture patterns described in the next section.

Texture and Motion Contrast Natural images, contain many texture patterns that are more complex and irregular than simple lines and edges. Studies of neural responses to textures have revealed a number of interesting properties that are not readily predictable from studies based on simpler visual stimuli. For example, many neurons are strongly influenced by texture patterns lying outside the classical receptive field, in that the surround pattern modulates the response to a central target even though the surround is ineffective on its own (Allman, Miezin, & McGuinness, 1985). Such modulatory effects have been found with static as well as moving texture patterns (Van Essen et al., 1989; Knierim and Van Essen, 1992).

General Comments

Despite the vast amount of experimental data available on the neurophysiology of V1, there are several fundamental issues about its function that remain largely unresolved. One issue concerns the sharpness of anatomical and physiological classifications. In many cases it is not known to what extent various compartments, cell types, and receptive field types represent biologically discrete groupings rather than points along a biological continuum. Another issue concerns the relationship between various receptive field properties (e.g., wavelength selectivity or direction selectivity) and their roles in perception (e.g., color or motion perception). For instance, recognition of the color of an object must surely rely on the activity of many wavelength selective neurons, but it is misleading to assume the converse. Many wavelength selective neurons may have alternative functions that are unrelated to color perception *per se* (cf. DeYoe & Van Essen, 1988; Dobkins & Albright, 1993; Van Essen & DeYoe, 1993). Finally, our description of cortex thus far has dealt only with static, hardwired aspects of processing. Dynamic aspects of processing that may occur in Vl and elsewhere will be discussed separately.

INFORMATION FLOW THROUGH VISUAL CORTEX

Current ideas about the functions of extrastriate visual cortex are guided by several broad principles, including the notions of hierarchical organization, concurrent processing streams, and highly distributed networks of information flow. These principles are derived from a combination of anatomical studies of the pathways for information flow, physiological studies of receptive field properties in different areas, and behavioral studies of the effects of selective lesions.

Each visual area is richly interconnected with other cortical areas and with subcortical nuclei, particularly the pulvinar complex (and also the LGN in the case of V1). In general these linkages are reciprocal, or bidirectional, in nature. Typically, each area is strongly interconnected with 5-10 other cortical areas, and there are usually several minor pathways as well (Felleman & Van Essen, 1991). At the low end of the spectrum, area V1 has major connections with only three cortical targets (areas V2, V3, and MT, in particular). At the high end, area V4 is connected with 21 other areas, and most of these pathways are reasonably robust.

The total number of identified pathways among 32 cortical areas related to vision is 305 (Felleman & Van Essen, 1991). If visual cortex were a fully interconnected matrix (i.e., if each area were linked to all others), there would be 32 x 31 = 992 pathways. Thus, the number of identified pathways is currently about one-third the theoretical limit and may reach 45-50% once all have been identified.

Hierarchical Organization and Concurrent Processing Streams

Several lines of anatomical and physiological evidence suggest that information processing in the cortex is fundamentally hierarchical in nature (Rockland & Pandya, 1979; Van Essen & Maunsell, 1983). By this, we mean that each area, and each cell population within an area, represents a particular stage of analysis relative to all other components in the system. However, this is neither a strictly serial scheme nor a strictly feedforward model involving only unidirectional information flow. Rather, there is extensive feedback as well as parallel processing, both of which are fully compatible with hierarchical organization in the broad sense.

The original version of the cortical hierarchy included thirteen visual areas interlinked by thirty-six different pathways (Van Essen & Maunsell, 1983). As more areas and pathways have been identified, the hierarchy has been extended to incorporate the new data. The most recent versions of the hierarchy (Felleman & Van Essen, 1991; Van Essen, Anderson & Felleman, 1992) span ten cortical levels of processing, as well as several subcortical levels, and extend all the way from the retina to the outputs from the visual system in limbic areas of the temporal lobe (entorhinal cortex, the hippocampus, and the amygdala). For simplicity, we will not illustrate the full scheme, but rather a version that involves only the few key areas previously identified on the cortical map. Thus, Figure 9 shows two subcortical stages (retina and LGN); area V1 is the first cortical stage; areas V2, V3, V4, and MT represent intermediate cortical stages; and the inferotemporal and posterior parietal complexes represent the highest cortical stages.

This figure also illustrates the concurrent processing streams that are discernible at both subcortical and cortical levels of the hierarchy. At subcortical levels, there is a distinctive population of very small (koniocellular) neurons in the LGN that constitute a third processing stream, separate from the M and P streams that have already been extensively discussed. This koniocellular (K) stream receives major inputs from the superior colliculus (SC) as well as from small-caliber axons of presumed retinal origin (cf. Casagrande and Norton, 1991).

At the cortical level, there are again three major streams, but these are not simply one-to-one continuations of the subcortical M, P, and K streams. They have been described as the MD (magno-dominated), BD (blob-dominated), and ID (interblob-dominated) streams, which are established in V1 and can be followed through several additional stages of the cortical hierarchy (Van Essen and DeYoe, 1993). The MD stream, which includes layers 4Cα and 4B in V1, appears on both anatomical and physiological grounds to be dominated by inputs from M cells in the LGN (Lachica, Beck, and Casagrande, 1992; Maunsell ref). The BD stream receives convergent inputs directly or indirectly from M, P, and K cells of the LGN (Lachica et al., 1992; Casagrande and Lachica, 1992). Selective inactivation of LGN layers has provided physiological confirmation that the CO blobs in V1 are strongly influenced by both M and P inputs (Nealey and Maunsell, 1991; Nealey, Ferrera and Maunsell, 1991), but the degree of physiological influence from the K stream remains to be established. The ID stream receives strong anatomical inputs preferentially relayed from P cells of the LGN, but selective inactivation studies indicate that CO interblob regions in V1 are strongly influenced by M cells (Nealey et al., 1991) via anatomical pathways yet to be determined.

In extrastriate cortex, the three processing streams are represented by a set of CO stripes in V2 (thick stripes, thin stripes, and interstripes) and at higher stages by a combination of distinct areas and compartments within areas. More specifically, the MD stream includes the thick stripes of V2, plus V3, MT, and areas in the posterior parietal complex. The BD stream includes the thin stripes of V2 and a set of compartments in V4 and posterior inferotemporal areas that

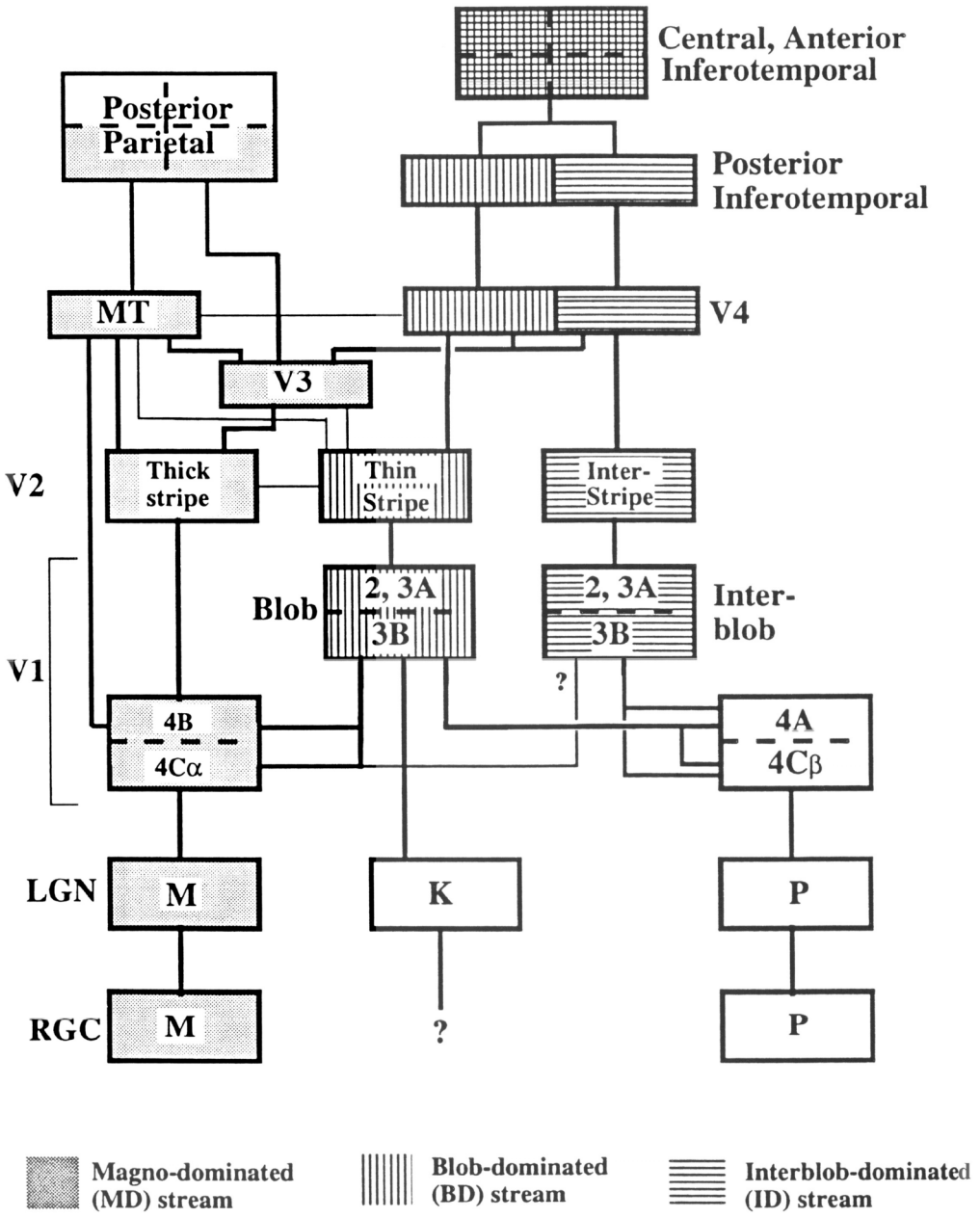

FIGURE 9 Hierarchical and compartmental organization of the visual pathway. This scheme illustrates information flow involving two subcortical levels and four cortical levels. Each of the lines between boxes represents a reciprocal pathway, and (except for the retino-geniculate projection) feedback connections are typically as robust as forward connections. Parallel processing is manifested at subcortical levels by the distinction amoong P, M, and K cells. In the cortex, there is convergence and divergence leading to three streams (MD, BD, and ID) that involve anatomically distinct compartments within V1, V4, and posterior inferotemporal cortex, as well as separate areas V3, MT, and areas of the posterior parietal complex streams.

cannot as yet be distinguished by their architecture. The ID stream includes the interstripes of V2 and the complementary set of compartments in V4 and posterior inferotemporal areas. Note that there is cross-talk between streams at several levels, even though they remain disguishable by virtue of the dominant anatomical projections (DeYoe and Van Essen, 1988; Zeki and Shipp, 1988; Felleman and Van Essen, 1991; Merigan and Maunsell, 1993; Van Essen and DeYoe, 1993).

Physiologically, cells in the MD stream tend to be selective for stimulus direction, disparity, and orientation, but not for stimulus wavelength. These regions also tend to be heavily myelinated, which should contribute to fast axonal

conduction velocities and enhance the capacity for carrying information at high temporal frequencies. The ID stream is characterized by a high incidence of orientation selectivity and end-stopping. Some cells are also selective for wavelength and binocular disparity, although there are discrepancies in the reported percentages of such cells (cf. DeYoe & Van Essen, 1988; Peterhans & von der Heydt, 1993) Cells in the BD stream tend to be selective for stimulus wavelength and also for low spatial frequencies (Tootell, Silverman, Hamilton, Switkes, & De Valois, 1988). Hence, it is natural to suspect that this stream plays an important role in color perception (Livingstone & Hubel, 1988b Zeki & Shipp, 1988). On the other hand, the various components of the BD stream are prominent in New World monkeys such as the owl monkey, which have little or no color vision. Moreover, it seems unlikely that color processing should exclusively occupy a large fraction of cortex, given that color information is such a small fraction of the information content we derive from natural images. Hence, it is likely that the BD stream is involved in other computational tasks, such as the analysis of brightness, surface textures, and/or shape based on shading cues.

Overall, these findings make sense, given what is known about the visual functions of the temporal and parietal lobes. As noted already, inferotemporal cortex has been implicated in pattern recognition and object identification (the "what" pathway) based on the behavioral deficits occurring after lesions and on the presence of neurons selectively responsive to faces and other complex patterns (Perrett, Mistlin, & Chitty, 1987; Miyashita, 1993). It is logical that these functions should rely primarily on the high-resolution. spectrally coded information carried by the BD and ID streams. However, it is also appropriate that the MD stream should contribute to object identification, in order to enhance our ability to recognize moving objects (structure from motion) and objects having very low contrast.

Posterior parietal cortex has been implicated in the analysis of spatial relationships (the "where" pathway) and in the control of eye movements and of visual attention (Ungerleider & Mishkin, 1982; Posner & Presti, 1987; Andersen, Snyder, Li, & Stricanne, 1993). It is not surprising that these processes should rely heavily on the information coming from the MD stream, with its high sensitivity to movement and change. However, it also makes sense for the BD and ID streams to contribute to these processes in order, for instance, to facilitate the analysis of spatial relationships among objects that are stationary or moving very slowly in the visual field.

In general. it seems unlikely that each processing stream simply handles the analysis of a single sensory cue (e.g., wavelength or velocity) for the purpose of contributing to a single aspect of perception. Rather, the cortex evidently acts as a concurrent processing system in which each stream carries out several interrelated tasks. For these tasks, each stage needs a diverse set of inputs and distributes its outputs widely for subsequent stages of analysis (DeYoe & Van Essen, 1988; Van Essen and DeYoe, 1993).

Functionality of Different Cortical Layers

Each of the cellular layers within the cortex is distinctive in its connectivity and its neuronal architecture. How, then, do the layers differ from one another in their functions? One possibility is that all layers employ similar processing strategies, and that lamination is a simple way of stacking several closely related processing sheets on top of one another in order to minimize connection lengths. For example, it is often tacitly assumed that the different layers of visual cortex share a common function of processing ascending sensory signals in order to extract information about the presence of various features. We will refer to this as *data analysis;* it is exemplified by orientation selectivity, direction selectivity, and other emergent receptive field properties of cells in V1 that reflect transformations of the properties of LGN cells.

In addition to data analysis, there are other computational problems that must also be faced in order to insure proper cortical function. One that we suspect is of great importance involves the *dynamic routing* of information into and out of each cortical area. Dynamic control of information flow is critical for the operation of standard digital computers, and analogous principles may apply to the nervous system as well. Support for this notion arises from a variety of physiological, psychophysical, and computational considerations. These have been articulated elsewhere in the context of specific strategies that might be involved in stereoscopic depth perception, motion analysis, and directed visual attention (Anderson & Van Essen, 1987; Van Essen & Anderson, 1990). Here we present the issue in a broader context that relates to the functionality of different cortical layers, irrespective of the particular cortical area in which they reside.

Our basic hypothesis is that the laminar organization of cortex reflects a tripartite division of labor, in which the data analysis stage is handled mainly within the superficial cortical layers; the middle layer (layer 4) is involved primarily in the gating or modulation of inputs for distribution to the superficial layers; and the deeper layers mediate the control of this selection and routing process. We note from the outset that the hypothesis is speculative and is intended only as a first approximation to a fundamentally complex network. However, if even approximately correct, it has major implications for our understanding of information flow within the cortex.

Figure 10 schematically illustrates seven pathways for information flow within and between cortical areas. The black arrows are presumed to be data pathways that represent various transformations of the original image data arising from ascending information flow (left) or descending flow (right). Others (stippled arrows) reflect putative "control pathways" whose role is to regulate information flow along the data pathways (cf. Baron, 1987). The first stage (A) represents the entry of ascending inputs to the cortex, which terminate mainly within layer 4 but also have a minor spin-off into layer 6. For most areas, the ascending inputs originate from other cortical areas at lower hierarchical stages, but for V1 (or other primary sensory areas) the inputs are from the LGN (or other thalamic relay nuclei).

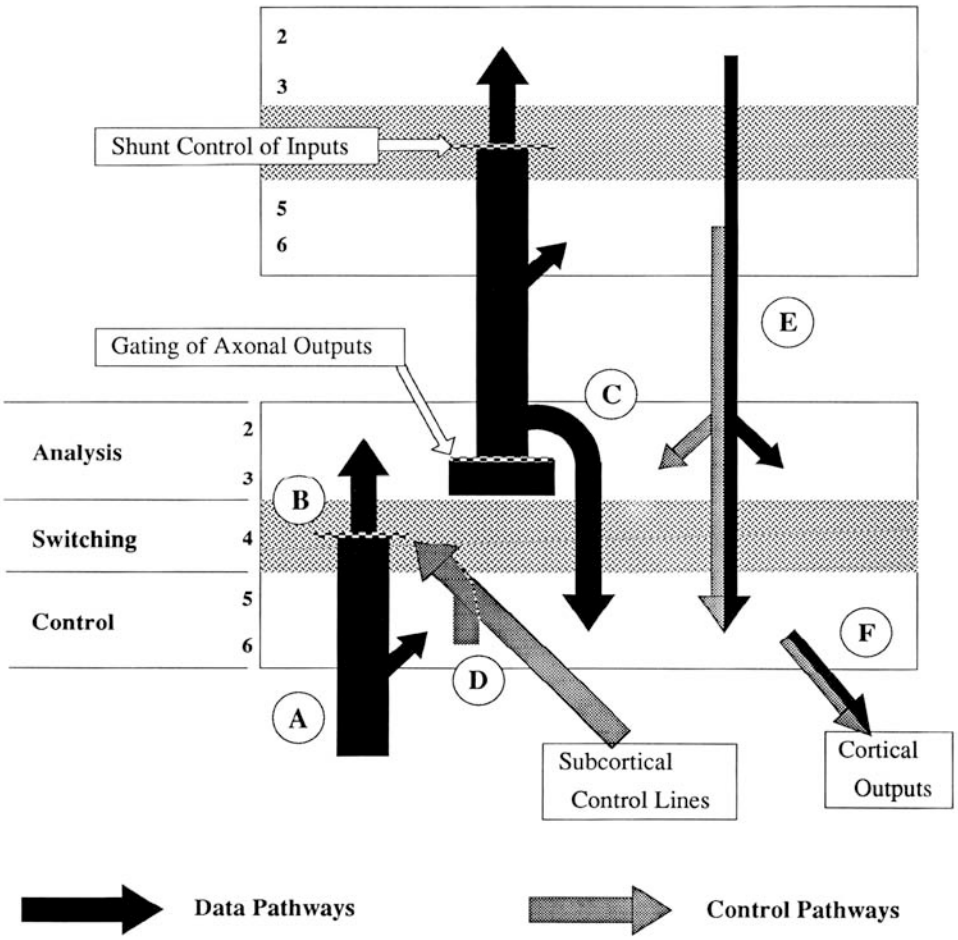

FIGURE 10 Proposed functionality of cortical layers. Arrows show the major routes of information flow within and between cortical areas as revealed by pathway tracing studies. Seven major stages can be distinguished, whose putative functions are suggested below. A. The cycle starts with ascending data from lower centers. B. Dynamic switching and filtering occurs within layer 4. (For area V1, this refers only to the geniculo-recipient layers 4A and 4C; layer 4B is considered one of the superficial layers in this context.) C. Data analysis occurs within the superficial layers, and the outputs are distributed to deeper layers within the same area and to layer 4 within higher areas. D. Appropriate control signals are generated within deep layers and in subcortical centers and are used to dynamically regulate the modulation process in layer 4. E. Descending signals (representing both data and control pathways) originate in both deep and superficial layers of a higher area and terminate in deep and superficial layers of a lower area, selectively avoiding layer 4. F. Cortical outputs are generated within the deep layers and are distributed to numerous subcortical centers.

Layer 4 provides major ascending projections to the superficial layers. We suggest that layer 4 acts as a gating network, in which only a subset of the ascending inputs to the superficial layers are enabled at any given moment. This is schematized by the reduction in the size of the arrows between inflow and outflow from layer 4, reflecting a dynamic input selection process at locus B. A possible cellular mechanism for this putative gating process involves shunting inhibition of the dendrites of neurons within layer 4 (Koch, Poggio. & Torre, 1983; Anderson & Van Essen, 1987). It is controversial whether shunting inhibition actually occurs in visual cortex, though (Ferster & Jagadeesh, 1992). An alternative mechanism for achieving a similar outcome might involve non-linear interactions among excitatory inputs, such as those mediated by NMDA receptors (Koch & Poggio, 1992).

Within the superficial layers, various types of data analysis are carried out, as appropriate for the particular area under consideration. The outputs of the superficial layers (C) include intrinsic projections to the deep layers within the same area and also extrinsic projections to higher cortical areas. These outputs may undergo another stage of selective gating which could be mediated by direct inhibition of axonal activity mediated by specialized cells known as chandelier cells (Somogyi, Freund, & Cowey, 1982; Schneider, 1985).

There are several possible sources for the putative control signals needed to determine how information is to be routed from one layer to the next. One major source (D) is layer 6, which provides feedback to layer 4 (Fitzpatrick et al., 1985). For extrastriate cortex, another source is the projection arising from the pulvinar nucleus (Benevento & Rezak, 1976; Ogren & Hendrickson, 1977). Finally, feedback from higher areas (E) could help regulate the axonal gating process hypothesized to occur in the outputs from superficial layers.

All cortical areas have major outputs to numerous subcortical structures in the thalamus, midbrain, and brainstem (including, for example, the pulvinar, LGN, superior colliculus, basal ganglia, and pons). In general these arise from cells in the deep cortical layers (F). Some of these pathways may represent feedback, whereas others may represent control pathways that feed directly into components of the motor system mediating eye, head, and limb movements.

The gating process in layer 4 presumably should operate in a coordinated fashion among neighboring cells. For example, in some situations it would be desirable to carry out a dynamic remapping process, involving translational shifts between the inputs and outputs of layer 4 mediated by a neural shifter circuit. We think that such a circuit could be constructed in a biologically plausible fashion and could aid in the solution of basic computational problems arising in the analysis of both motion and depth information (Anderson & Van Essen, 1987; Van Essen & Anderson, 1990). Analogous types of gating could be used for dynamic scaling and for remapping at higher stages in relation to directed visual attention (Olshausen, Anderson, and Van Essen, 1993; Van Essen, Olshausen, Gallant, Press, Anderson, Drury, Carman, & Felleman, 1993). These can in general be regarded as reformatting operations that condition the input data prior to transmission to superficial layers.

The shifter hypothesis explicitly predicts that neuronal receptive fields should not be rigidly locked to absolute retinal coordinates, even at the earliest stages of visual cortex. Rather, receptive fields should shift in position over a significant range, in a manner dictated by motion, depth, or other types of information arising outside as well as inside the classical receptive field of the cells. The magnitude of these shifts should be very small at the initial stage, but would become larger at progressively higher stages of the cascade.

Evidence for dynamic shifts in sensory receptive fields has been reported in the primate superior colliculus (Jay & Sparks, 1984) and in area V4 and inferotemporal cortex (Moran & Desimone, 1985; Connor, Gallant, and Van Essen., 1993). For V1 the evidence is mixed as to whether dynamic receptive field shifts occur, with some evidence in support of the hypothesis (Motter & Poggio, 1988) and some evidence against (Gur & Snodderly, 1987).

The functional assignments we have proposed for different layers should not be regarded as rigid and all-or-none. For example, layer 4 of area V1 is likely to make some contribution to the data analysis stage in addition to whatever role it has in dynamic switching. This is suggested by the presence of significant numbers of orientation selective cells in

layer 4Ca (Blasdel & Fitzpatrick, 1984). Also, a high incidence of orientation selectivity and even direction selectivity is found in layer 4 of V1 in the cat (Gilbert. 1977), suggesting that there are important species differences in laminar processing. For the superficial layers, we have already noted that they might carry out some dynamic switching functions in addition to their role in data analysis.

Despite this blurring of laminar distinctions, our basic hypothesis remains a simple one: a primary function of layer 4 is to regulate the incoming data in order to improve the efficiency and flexibility of computation in the superficial layers and to coordinate processing across cortical areas. Within this general framework, it is important to formulate specific experimental paradigms that can critically test the validity of the hypothesis and its generality across different species and different cortical areas.

Cortical Microcircuitry and Cascaded Network Architecture

The preceding two sections concentrated on information flow and neural representations in different areas and cortical layers. We now turn to a finer-grained analysis dealing with several aspects of the microcircuitry that underlies specific receptive field properties.

Each cortical neuron typically receives between 10^3 and 10^4 synapses, and there is evidence that these usually reflect weak connections from hundreds or thousands of other neurons rather than massive inputs from just a few neurons (Braitenberg, 1978). Thus, there are literally millions of neurons that are only a few synaptic stages away from any given cortical cell. In this respect, the cortex is clearly a highly distributed neural network, and it may be profitable to apply some of the modeling approaches that have recently been applied to artificial neural networks. To make such models explicit and biologically realistic, it is important to know the spatial extent and relative strength of the major inputs and outputs of each cortical layer and each neuronal cell type, along with the degree of divergence and convergence as information flows in both directions through the cortical hierarchy. One useful way of representing some of these relationships is a connectivity matrix, analogous to those often used to illustrate connections in artificial neural networks (e.g., Hopfield, 1984). Two examples will be given using this approach, one concerning processing in the M stream and the other concerning visual attention and the pathway from V1 to IT.

A Connectivity Matrix for the M Stream

Figure 11 illustrates a connectivity matrix that covers several processing stages within the M stream, including the magnocellular layers of the LGN, layers 4Ca and 4B of V1, and area MT. The basic format is illustrated in the inset on the upper right. It involves a one-dimensional array of neurons whose cell bodies are aligned in a vertical row along the *y* axis; for simplicity, only two neurons (*i* and *j* are drawn. The inputs to each neuron impinge on a target dendrite that runs horizontally to the right of the cell body. Each neuron also has an axon that loops around and runs vertically, acting as a source that intersects with the dendrites of all neurons The intersection between the axon of neuron i and the dendrite of neuron j is a synapse whose strength can be denoted as w_{ij}. More generally, the inputs to a given cell can be found by examining the synaptic weights along the appropriate row, and its outputs by examining the appropriate column.

In applying this analysis to the M stream, we create a one-dimensional array by imagining a line running along the representation of the horizontal meridian within each visual area. The entire visual representation, from fovea (F) to periphery (P), is included for each area, and successive hierarchical stages (LGN, V1-4Ca, V1-4B, and MT) are placed next to one another along each axis. Each rectangular region within the overall matrix represents a single extrinsic or intrinsic pathway. Obviously on such a coarse scale individual cells, axons, and connections cannot be resolved. For simplicity, we have used stippling to indicate regions where extensive synaptic contacts are made. These regions tend to run along diagonal bands within each rectangle, and the width of the band reflects the physical extent of divergence in the pathway. For example, the projection from the LGN to layer 4Ca of V1 is tightly organized topographically, insofar as individual magnocellular LGN axons arborize over a 1-mm zone within the 40-mm linear extent of V1 (narrow rectangle along far lower left). A comparable spread occurs in the intrinsic connections within layer 4Ca (large

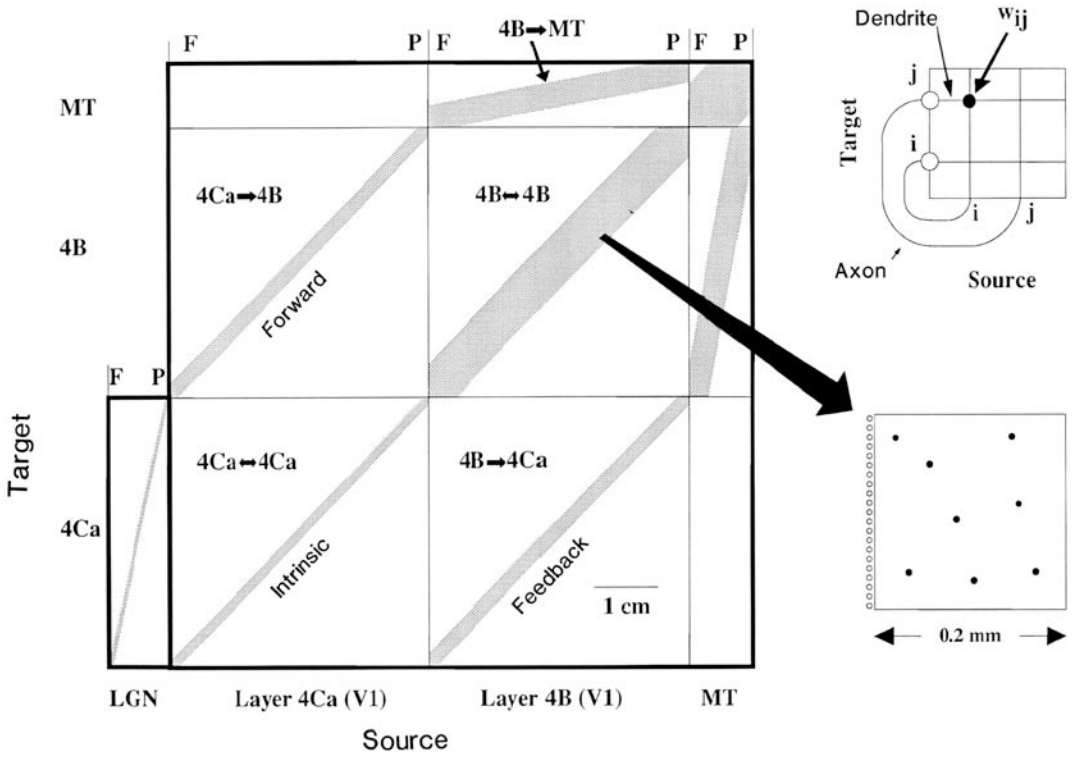

FIGURE 11 A connectivity matrix for representing circuitry within and between cortical areas. The inset on the upper right shows the format for representing connections within a one-dimensional array of neurons. The axes of the matrix are arranged to represent information flow from a source along the *x* axis to a target along the *y* axis. In neurobiological terms, cell bodies are arrayed along the *y* axis, with dendrites running horizontally and axons curving around to run vertically. The main part of the figure shows a connectivity matrix for a one-dimensional slice through several major subdivision of the M stream. The *x* axis represents, in sequence, the axonal outputs of the LGN (magnocellular layers), layers 4Ca and 4B of V1, and area MT; the*y* axis represents the inputs to layers 4Ca and 4B of V1 and to MT. Stippling indicates zones within which connections actually occur. Circuitry intrinsic to each area lies along the main diagonal through the matrix: feedforward pathways lie above and to the left, whereas feedback pathways lie below and to the right. This scheme does not show the ocular dominance stripes in layer 4C, but these and other features could readily be incorporated in a more refined version.

square in lower left) and in the projection from 4Ca to 4B, one square above (Blasdel, Lund, and Fitzpatrick,, 1985; Fitzpatrick et al., 1985). Greater divergence occurs at higher stages, so that MT receives ascending inputs from a substantial portion of the visual field, and its intrinsic connections (small square, far upper right) actually cover most of the representation. These anatomical features reflect the gradual erosion of topography as indicated by increases in classical receptive field size at progressively higher stages of the hierarchy. Feedback pathways, represented in rectangles along the lower right of the matrix, suggest an anatomical basis for the modulatory surround effects that have been demonstrated well outside the classical receptive field (Allman et al., 1985; Knierim & Van Essen, 1992).

The connectivity matrix can also be used to illustrate the actual density of synapses seen at a much finer grain. The inset on the lower right shows an expanded l-mm segment from layer 4B. We estimate that only a small percentage of the total possible connections are actually present, making this a rather sparsely interconnected network.

Connectivity matrices can represent a wealth of anatomical detail in a way that can be related to information flow within and between areas. This provides a framework for generating models aimed at simulating specific aspects of network processing in the cortex (cf. Wehmeier, Dong, Koch, & Van Essen, 1989; Wilson & Bower. 1989). As more information about the extent and density of specific connections becomes available, the connectivity matrix can be refined to show much greater detail than the first-cut approximations shown here.

Inferotemporal Cortex and Directed Visual Attention

Discrimination and identification of complex patterns (e.g., faces) occurs readily over a wide range of positions, scales, and orientations. The underlying neural mechanisms are not well understood, but there is psychophysical and physiological evidence suggesting that pattern recognition is intimately related to the processes of figure/ground segregation and directed visual attention (Rolls & Baylis, 1986; Baron, 1987; Wise & Desimone, 1988; Van Essen et al., 1991). During attentive scrutiny, we can shift both the location and the spatial scale of the region of the visual field that is attended. Several observations suggest that the effective window of integration extends over about 15-30 resolvable steps (sampling nodes), irrespective of retinal position and the spatial scale of the analysis (Virsu & Rovamo, 1979; Jamar & Koenderink, 1983; Toet, van Eekhout, Simons, & Koenderink, 1987; Van Essen et al., 1991).

An attractive model for this process involves dynamic control of information flow into inferotemporal cortex (Anderson & Van Essen, 1987; Baron, 1987; Olshausen et al., 1993). In essence, the idea is that IT receives functionally effective inputs from only a limited portion of the retina, which varies from moment to moment and reflects the size and position of the window of attention. Figure 12 illustrates a modified version of our earlier model for routing of inputs related to visual attention. It involves a connectivity matrix that extends from V1 through V2, V4, and IT. The representation is highly simplified in several respects: it ignores the various compartmental and laminar subregions in V1, V2, and V4; it treats IT as a single area; and it ignores the intrinsic connections within each area.

The representation of the visual field is very sharp in V1, but it becomes eroded by the divergence of feedforward connections at each successive stage. As a consequence, each cell in IT has anatomical inputs that span nearly the entire retina. In keeping with this, receptive fields of IT neurons are known to be very large in anesthetized animals, often covering most of the visual field (Desimone & Gross, 1979). In alert animals, however, receptive fields tend to be restricted to the immediate region to which the animal is attending (Moran & Desimone, 1985) and that they can shift with the position (but perhaps not the scale) at which attention is directed (Connor et al., 1993). This suggests that most of the physically available inputs to IT neurons are functionally ineffective in the alert animal, and that the effective inputs can be shifted dynamically in concert with changes in attention. This process is symbolized by the blackened regions within each of the diagonal bands in Figure 12. These represent subsets of enabled connections within the overall matrix which can give rise to a window of attention in a particular part of the visual field. Other connections are presumed to be rendered ineffective through the opertion of control circuitry discussed earlier (cf. Figure 10).

The way this scheme works can be visualized by tracing the cascade of activity arising from neurons in V1 within the small window from *a1 to b1* shown on the lower left. This activates a set of neurons in V2 between points *a2* and *b2* and neurons in *V4* between *a4* and *b4*. Finally, this leads to a mapping across all of IT. The window of attention can be changed in position or scale by appropriate alterations in the pattern of effective connectivity at each stage, which would be mediated by top down control signals rather than directly from ascending sensory inputs. Translations of the blob-like activated domains within the connectivity matrix would lead to shifts in the retinal position of the window; changes in orientation of the domains would modulate the effective size of the window. In the reverse direction, the receptive field of single neurons in IT and *V4* can be mapped back to a small region within V1, which would change systematically when the window of attention is shifted.

In this simplified scheme, control of the routing process would require use of inhibitory circuitry to sculpt the position, orientation, and thickness of the activated domains that gate information flow through each pathway. More complex operations can be imagined, though, which could allow these domains to be curved, thereby warping the image representation. There might also be mechanisms for selection on the basis of cues other than position (such as depth or chromatic cues, Motter, 1992). The high-level control signals needed to mediate these processes might originate in the parietal lobe, frontal lobe, superior colliculus, and/or pulvinar, all of which have been implicated in the control of visual attention (Posner & Presti, 1987; Desimone, Wessinger, Thomas, and Schneider, 1990; Anderson & Van Essen, 1993).

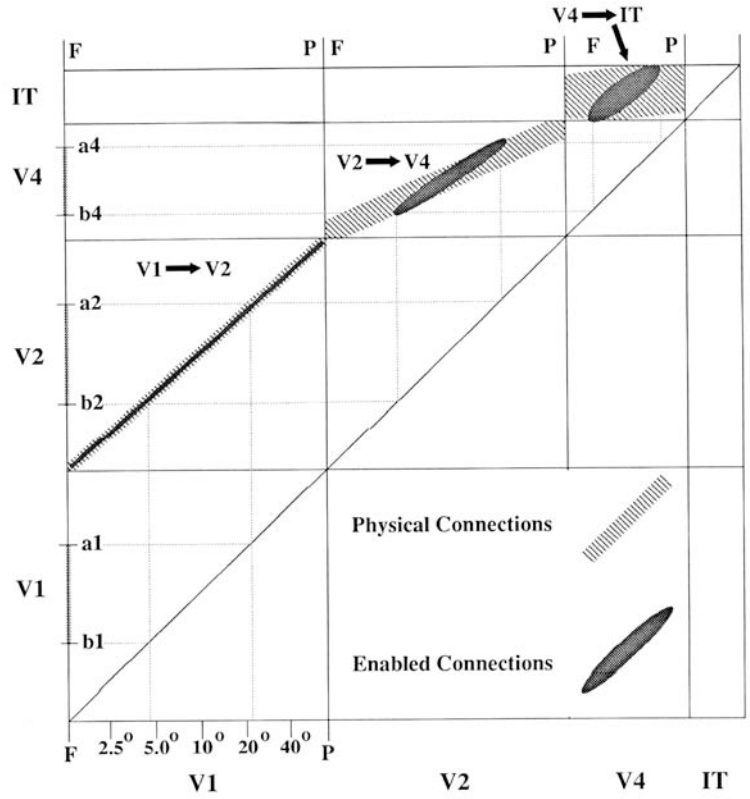

FIGURE 12 A circuit that could mediate directed visual attention, illustrated using a connectivity matrix leading from V1 to IT. For simplicity, only feedforward connections are shown; feedback and intrinsic circuitry are ignored. Also, only one of the numerous visual areas within the IT complex is illustrated, but the scheme could be readily extended to the entire complex. The extent of physical connections subserving each pathway is shown by hatching. Connections that are enabled at a given moment are indicated by dark shading; the rest are presumed to be disabled by shunting inhibition or some other non-linear mechanism. The fine dotted lines allow one to trace the flow of information from a restricted portion of V1 (between points a1 and b1 on the left side of the matrix) to the entirety of IT. This divergence arises mainly from the gating postulated for the V2 to V4 and V4 to IT pathways, but it is useful to track the flow in a bottom-up sequence. Information flow from V1 to V2 involves relatively little divergence. The activated connections shown here occupy a narrow strip along the center of the band of physical connections. Consequently, V1 is mapped onto V2 in an orderly fashion that largely preserves local topographic order. In particular, points a1 and b1 map respectively onto a2 and b2. Shifting the band of activated connections would produce a small amount of translation in the mapping, while broadening the band would blur the mapping by coupling each neuron in V2 to a wider area of V1. The mapping from V2 to V4 involves a zone of activated connections that is tilted relative to the diagonal formed by the physical connections. This has the consequence of expanding the representation of the region within the window of attention at the expense of the remainder of the representation: segment a4-b4 occupies a larger fraction of V4 than the a2-b2 segment does in V2. [n going from V4 to IT, the zone of activated connections once again has an oblique orientation, which leads to all of IT being filled by the mapping from segment a4-b4. Working backward through the cascade demonstrates that IT as a whole receives an orderly mapping from segment a1-b1 of V1, corresponding to a restricted window of attention. A similar analysis can be used to show that an individual cell in V4 or IT would have a restricted receptive field that shifts in accordance with changes in the window of attention. The size of the receptive field would reflect the aggregate amount of blurring that arises from the finite width of the activated zone at each level. Narrow zones would preserve positional information nation, whereas wider zones might achieve a better signal-to-noise by integrating across a larger domain. Neurons in V4 are known to be responsive when the animal is not attending or is attending a target outside the receptive field of the cell (Moran & Desimone, 1985). Presumably, this means that many of the connections serving regions outside the window of attention (i.e., outside the a4-b4 segment) are activated, rather than being suppressed as shown in the figure for the sake of graphical clarity (see Olshausen et al., 1993). This diagram illustrates only the mapping within one hemisphere, corresponding to one visual hemifield. The scheme can readily be extended to cover both hemispheres and the full visual field. Extensive interhemispheric connections exist in extrastriate visual cortex, particularly at higher levels, which provides the anatomical basis for smooth integration across the entire visual field. Alternative schemes for obtaining coordinate transformations in inferotemporal cortex could be generated using this basic mapping scheme. For example, the representation in IT might be based on image segmentation and object-centered coordinates (cf. Baron, 1987). In that case, the mapping in IT would cover the region of the visual field corresponding to whatever is perceived as the "figure" in tasks of figure-ground segregation (a face, for example) even if the window of attention were involved in scrutiny of only portions of the object (e.g., the eyes and nose).

This discussion is intended only to outline some the possibilities for selective routing of information from the retina into the temporal lobe. There are numerous details to be worked out to establish this a complete model of attentive processing (Olshausen et al., 1993), and many additional experiments are needed to establish whether the cortex indeed operates according to this strategy. There may be interesting generalizations to other sensory modalities, and to cognitive processing and motor control (Van Essen et al., 1993). There are also potential clinical implications, because some neurological and psychiatric disorders (e.g., dyslexia and schizophrenia) conceivably could reflect malfunctions in the circuitry involved in the dynamic control of information flow.

CONCLUDING REMARKS

In this chapter, we have reviewed many types of information about the anatomy and physiology of the primate visual system, and we have tried to place these data into the framework of systems-oriented computational models of visual processing. We believe that this type of interdisciplinary approach is crucial for any deep understanding of biological vision and for constructing successful artificial vision systems. Progress in this endeavor can be facilitated by bearing in mind several general points.

1. *Progressive complexity*. Model building is fundamentally an iterative process, in which the models become more elaborate and complex in order to account more fully for the biological data. One cannot realistically expect full-scale models at the outset, but neither should one remain satisfied with using simple, qualitative schemes to account for the richness of biological systems.

2. Good engineering. Models should respect principles of good engineering. A model may be only as strong as its weakest engineering link. In this respect, it is important to specify what aspects of function a model is intended to simulate or represent. For sensory systems it is also important to ascertain how *successful* the model is in preserving information available in the raw sensory data. Once lost, information cannot be regained, and there should be a clear rationale when such losses occur in a model.

3. *Predictive nature*. Models that make strong, experimentally testable predictions have been relatively rare in neurobiology, which largely accounts for the lack of appreciation of neural modeling approaches in some quarters. There is a clear need for models that are cast in explicitly neurobiological terms, so that they can be closely related to experimental data. One of the reasons we find the shifter hypothesis attractive is because of the specific predictions it makes about the dynamic nature of receptive fields. Models of this type can advance our understanding, whether or not they eventually turn out to be correct in detail.

4. *Relevance to image processing*. Artificial vision systems must cope with problems that are fundamentally similar to those successfully met by biological vision systems after millions of years of evolution. In connection with this, models of visual processing provide an important two-way link between the fields of biological vision and computer vision. Models developed in the study of biological vision can guide the fabrication of devices designed to extract useful information from complex natural images (cf. Mahowald & Mead, 1988). Principles derived from computer vision can in turn guide the formulation of models that represent specific biological processes. This interplay will in the long run serve as a powerful impetus to progress on both fronts.

Acknowledgments

Work from this laboratory was supported by ONR contract N00014-89-J-1192 and by the McDonnell Center for Higher Brain Function at Washington University. We thank many of our colleagues for valuable discussions and S. Danker for help in preparation of the manuscript.

Adelson, E. H.. & Bergen, J. (1985). Spatiotemporal energy models for the perception of motion. *Journal* of *the Optical Society of America, 2,* 284-299.

Adelson, E. H.. & Bergen, J.R. (1991) The plenoptic function and the elements of early vision. In: *Computational Models of Visual Processing*, M. Landy, J. Movshon, ed., MIT Press, 1991.

Allman, J., Miezin. F., & McGuinness, E. (1985). Stimulus specific responses from beyond the classical receptive field: Neurophysiological mechanisms for local-global comparisons in visual neurons. *Annual Review of Neuroscience,* 8, 407-430.

Andersen, R. A. (1989). Visual and eye movement functions of the posterior parietal cortex. Ann. Rev. Neurosci. 12, 277-403.

Andersen, R. A., Snyder, L. H., Li, C.-S. & Stricanne, B. (1993).Coordinate transformations in the representation of spatial information. *Current Opinion in Neurobiology,* 3, 171-176.

Anderson, C. H. (1986). The transmission of information in X and Y ganglion cells. *Investigative Ophthalmology & Visual Science. Suppl. 27,* 242.

Anderson, C. H., & Van Essen, D. C. (1987). Shifter circuits: A computational strategy for dynamic aspects of visual processing *Proceedings of the National Academy of Sciences of the United States of America,* 84, 6297-6301.

Anderson, C. H., and Van Essen, D. C. (1993). Dynamic neural routing circuits. In D. Brogan, A. Gale and K. Carr, (Eds), Visual Search 2. London: Taylor and Francis.

Atick, J. J, and Redlich, A. N (1992). What does the retina know about natural scenes?. Neural Computation 4, 196-210.

Baron, R. J. (1987). *The cerebral computer.* Hillsdale, NJ: Erlbaum.

Benevento, L. A.. & Rezak, M. (1976). The cortical projections of the inferior pulvinar and adjacent lateral pulvinar in the rhesus monkey *(Macaca mulatta):* An autoradiographic study. *Brain Research, 108,* 1-24.

Blakemore, C., & Vital-Durand, F. (1986). Organization and postnatal development of the monkey's lateral geniculate nucleus. *Journal of Physiology.* 380. 453-491.

Blasdel, G. G., & Fitzpatrick, D. (1984). Physiological organization of layer 4 in macaque striate cortex. *Journal of Neuroscience. 4,* 880-895.

Blasdel, G. G., & Lund, L. S. (1983). Termination of afferent axons in macaque striate cortex. *Journal of Neuroscience,* 3, 1389-1413.

Blasdel, G. G., Lund, L. S., & Fitzpatrick, D. (1985). Intrinsic connections of macaque striate cortex: Axonal projections of cells outside lamina 4C. *Journal of Neuroscience, 5,* 3350-3369.

Blinkov, S. M.. & Glezer. I.I. (1968) *The human brain in figures and tables* New York: Basic Books.

Braitenberg, V. (1978). Cell assemblies in the cerebral cortex. *Lecture Notes in Biomathematics. 21,* 171- 188.

Buchsbaum, G. (1987). Color Signal Coding: Color Vision and Color Television. *Color Research and Application* 12, 266-269.

Casagrande, V.A. and Lachica, E.A. (1992) What are the cytochrome (CO) blobs and interblobs really segregating? *Invest. Ophthal. & Vis. Sci. Suppl.* 33:900.

Casagrande, V.A. and Norton, T. T. (1991) Lateral geniculate nucleus: A review of its physiology and function: *Vision and Visual Dysfunction, Vol. 4, The Neural Basis of Visual Function*, A.G. Leventhal, ed., MacMillan Press.

Conley, M. and D, Fitzpatrick, 1989, Morphology of retinogeniculate axons in the macaque. *Visual Neurosci.* 2:287-296.

Connolly, M., & Van Essen, D. (1984). The representation of the visual field in parvicellular and magnocellular layers of the lateral geniculate nucleus in the macaque monkey. *Journal of Comparative Neurology, 226,* 544-564.

Connor, C.E., Gallant, J.L. and Van Essen, D.C. (1993) Effects of focal attention on receptive field profiles in area V4. *Soc. Neurosci. Abstr.* 19:974..

Crick, F. (1984). Function of the thalamic reticular complex: The searchlight hypothesis. *Proceedings of the National Academy of Sciences of the United States of America,* 81, 4586-4590.

Crook, J. M., Lange-Malecki, 8., Lee, B. B., & Valberg, A. (1988). Visual resolution of macaque retinal ganglion cells. *Journal of Physiology,* 396, 205-224.

Dacey, D. M. and Petersen, M. R. (1992). Dendritic field size and morphology of midget and parasol ganglion cells of the human retina. Proc. Natl. Acad. Sci. USA 89, 9666-9670.

Daugman, J.G.(1985).Uncertainty relation for resolution in space, spatial frequency, and orientation optimized by two-dimensional visual cortical filters. *Journal of* the *Optical Society of America, 2, 11* 60-1169 .

De Monasteno, F. M. (1978). Properties of concentrically organized X and Y ganglion cells of macaque retina. *Journal of Neurophysiology, 41.* 1394-1417.

De Monasterio, F. M., & Gouras, P. (1975). Functional properties of ganglion cells of the rhesus monkey retina. *Journal of Physiology, 251,* l67-195.

De Monasterio, F. M.. McCrane, E. P., Newlander. J. K., & Schein, S. I. (1985). Density profile of blue-sensitive cones along the horizontal meridian of macaque retina. *Investigative Ophthalmology & Visual Science*. 26, 289-302.

Derrington, A. M.. & Lennie, P. (1984). Spatial and temporal contrast sensitivities of neurones in lateral geniculate nucleus of macaque. *Journal of Physiology,* 357, 219-240.

Desimone, R., & Gross, C. G. (1979). Visual areas in the temporal cortex of the macaque. *Brain Research,* 178, 363-380.

Desimone, R., Wessinger, M., Thomas, L., & Schneider, W. (1990) Attentional control of visual perception: Cortical and subcortical mechanisms. *Cold Spr. Harbor Symp. Quant. Biol.* 40,963-971.

DeValois, R. L., Albrecht, D. G., & Thorell, L. G. (1982). Spatial frequency selectivity of cells in macaque visual cortex. *Vision Research,* 22, 545-559.

DeValois, R.L. and DeValois, K.K. (1993) A multi-stage color model. *Vision Res.*, 33, 1053-1065.

DeYoe, E., Knierim, J., Sagi, D., Julesz, B., & Van Essen, D. (1986). Single unit responses to static and dynamic texture patterns in macaque V1 and V2 cortex. *Inv. Ophthalmology & Visual Science Suppl.,* 27, 18.

DeYoe, E A., & Van Essen, D. C. (1988). Concurrent processing streams in monkey visual cortex. Trends in *NeuroSciences,* 11,219-226.

Dobbins, A., Zucker, S. W., & Cynader, M. S. (1987). Endstopped neurons in the visual cortex as a substrate for calculating curvature. *Nature,* 329, 438-441.

Dobkins, K.R. and Albright, T.D. (1993) What happens if it changes color when it moves?: Psychophysical experiments on the nature of chromatic input to motion detectors. *Vision Res.* 33, 1019-1036.

Dowling, I. E. (1987). *The retina: An approachable part of the brain*. Cambridge, MA: Belknap.

Felleman, D. I ., & Van Essen, D. C. (1991). Distributed hierarchical processing in the primate visual cortex. *Cerebral Cortex* , 1, 1-47.

Ferster, D & Jagadeesh ,B (1992) EPSP-IPSP interactions in cat visual cortex studied with in vivo whole-cell patch recording. *J. Neurosci.* 12, 1262-1274.

Field, D. J. (1992). Scale-invariance and self-similar "wavelet" transforms: An analysis of natural scenes and mammalian visual systems. In Farge, M., Hunt, J. & Vassiclicos, J. C. (Eds), Wavelets, fractals and Fourier transforms: New developments and new appliations. Oxford: Oxford University Press.

Field, D. J. (1987). Relations between the statistic of natural images and the response properites of cortical cells. Journal of the Optical Society of America A, 4, 2379-2394.

Fitzpatrick, D., Lund, I. S., & Blasdel, G. G. (1985). Intrinsic connections of macaque striate cortex: Afferent and efferent connections of lamina 4C. *Journal of Neuroscience, 5,* 3329-3349.

Fukuda, Y, Sawai, H., Watanabe, M., Wakakuwa, K., and Morigiwa, K. (1989). Nasotemporal overlap of crossed and uncrossed retinal ganglion cell projections in the Japanese monkey (Macaca fuscata). The Journal of Neuroscience, 9, 2353-2373.

Gallant, J.L., Braun, J., and Van Essen, D.C. (1993) Selectivity for polar, hyperbolic, and cartesian gratings in macaque visual cortex. Science 259:100-103.

Gilbert, C. D. (1977). Laminar differences in receptive field properties of cells in cat primary visual cortex. *Journal of Physiology,* 268, 391-421.

Grünert, U., Greferath, U., Boycott, B.B., and Wässle, H. (1993) Parasol (Pα) ganglion-cells of the primate fovea: Immunocytochemical staining with antibodies against $GABA_A$-receptors. *Vision Res.* 33:1-14.

Gur, M., & Snodderly, D. M. (1987). Studying striate cortex neurons in behaving monkeys: Benefits of image stabilization. *Vision Research,* 27, 2081-2087.

Hicks, T. P., Lee, B. B., & Vidyasagar, T. R. (1983). The responses of cells in macaque lateral geniculate nucleus to sinusoidal gratings. *Journal of Physiology,* 337, 183-200.

Hopfield, I. I. (1984). Neurons with graded response have collective computational properties like those of two-state neurons. *Proceedings of National Academy of Sciences of the United States of America,* 81,3088-3092.

Hubel, D. H., & Wiesel, T. N. (1962). Receptive fields, binocular interaction and functional architecture in the cat's visual cortex. *Journal of Physiology,* 160, 106 154.

Hubel, D. H., & Wiesel, T. N. (1968). Receptive fields and functional architecture of monkey striate cortex. *Journal of Physiology, 195,* 215-243.

Hubel, D. H., & Wiesel, T. N. (1974). Uniformity of monkey striate cortex: A parallel relationship between field size, scatter, and magnification factor. *Journal of Comparative Neurology,* 158,295-306.

Hubel, D. H., & Wiesel, T. N. (1977). Functional architect macaque monkey visual cortex. *Proceedings of the Royal Society of London,* 198, 1-59.

Jamar. J. H. T., & Koenderink, J. J. (1983). Sine-wave gratings. Scale invariance and spatial integration at suprathreshold ct,q contrast. *Vision Research,* 23, 805-810.

Jay, M. F., & Sparks, D. L. (1984). Auditory receptive fields in primate superior colliculus shift with changes in eye position. *Nature,* 309. 345-347.

Jones, J. P., & Palmer, L. A. (1987). An evaluation of the two dimensional Gabor filter model of simple receptive fields in cs striate cortex. *Journal of Neurophysiology,* 58, 1233-1258.

Julesz, B. (1984). Towards an axiomatic theory of preattentive vision, In G. M. Edelman, W. E. Gall, & W. M. Cowan (Eds. *Dynamic aspects of neocortical function*. New York: Wiley,

Kaplan, E., Purpura, K., & Shapley, R. M. (1987). Contrast affects the transmission of visual information through the mammalian lateral geniculate nucleus. *Journal of Physiology, 39* 267-288.

Kaplan, E., & Shapley, R. M. (1982). X and Y cells in the lateral geniculate nucleus of macaque monkeys. *Journal of Physiology* 330, 125-143.

Knierim, J. J. and Van Essen, D. C. (1992) Visual cortex: cartography, connections, and concurrent processing. Curr. Op. Neurobiol., 2: 150-155.

Koch, C . (1987). The action of the corticofugal pathway on sensory thalamic nuclei: An hypothesis. *Neuroscience, U,* 399-406.

Koch, C. & Poggio, T. (1992) Multiplying with synapses and neurons. In: *Single Neuron Computation Neural Nets: Foundations to Applications*, Academic Press, pp. 315-345.

Koch, C., Poggio, T., & Torre, V. (1983). Non-linear interaction in a dendritic tree: Localization, timing and role in information processing. *Proceedings of the National Academy of Sciences of the United States of America,* 80, 2799-2802.

Koenderink, J. J., & van Doorn, A. I. (1978). Visual detection of spatial contrast; influence of location in the visual field, target~ extent and illuminance level. *Biological Cybcrnetics, 30,* 157-167.

Kosslyn, S. M. (1988). Aspects of a cognitive neuroscience of mental imagery. *Science,* 240,1621-1626.

Kruger, J. (1977). The shift-effect in the lateral geniculate body of; the rhesus monkey. *Experimental Brain Research,* 29, 387-391.

Lachica, E.A., Beck, P.D. and Casagrande, V.A. (1992) Parallel pathways in macaque monkey striate cortex: Anatomically defined columns in layer III. Proc. Natl. Acad. Sci. 89:3566-3570.

Laughlin, S. M. (1987). Form and function in retinal processing. . *Trends in Neurosciences,* 10, 478-483.
Lee, B. B., Virsu, V., & Creutzfeldt, O. D. (1983). Linear signal: transmission from prepotentials to cells in the macaque lateral geniculate nucleus. *Experimental Brain Research,* 52, 50-56.
Lee, B.B., Martin, P.R., & Valberg, A. (1989) Sensitivity of macaque ganglion cells to luminance and chromatic flicker. J. Physiol. 414,223-243.
Livingstone, M. S., & Hubel, D. H. (1984). Anatomy and physiology of a color system in the primate visual cortex *Journal of Neuroscience,* 4, 309-356.
Livingstone, M. S., & Hubel, D. H. (1988a). Do the relative mapping densities of the magno- and parvocellular systems vary with eccentricity? *Journal of Neuroscience,* 8, 4334-4339.
Livingstone, M.S., & Hubel, D. (1988b). Segregation of form, color, movement, and depth: Anatomy, physiology, and perception. *Science,* 240,740-749.
Lund, J.S. (1988). Excitatory and inhibitory circuitry and laminar mapping strategies in primary visual cortex of the monkey. In G. M. Edelman. W. E. Gall. & W. M Cowan (Eds.), *Signal and sense: Local and global order in perceptual maps* New York: Wiley
Mahowald, M.. & Mead. C. A (1988). A silicon model of early visual processing. *Neural Networks, 1,* 91 -97.
Marrocco, R. T., McClurkin, J.W., & Young, R. A. (1982). Spatial summation and conduction latency classification of cells of the lateral geniculate nucleus of macaques. *Journal of Neuroscience,* 2,1275-1291.
Merigan, W.H. and Maunsell, J.H.R. (1993) How parallel are the primate visual pathways? Ann. Rev. Neurosci. 16:369-402.
Michael, C. R. (1985) Laminar segregation of color cells in the monkey's striate cortex *Vision Research,* 25, 415-423.
Miyashita, M. (1993) Inferior temporal cortex: Where visual perception meets memory. *Ann. Rev. Neurosci.* 16, 245-264.
Moran, J., & Desimone, R (1985) Selective attention gates visual processing in the extrastriate cortex. *Science,* 229, 782-784.
Motter, B.C. (1992) Selective activation of V4 neurons in a color and orientation discrimination task. *Inv. Ophthalmol. & Vis. Sci. Suppl.* 33, 1131.
Motter, B. C.. & Poggio. G F (1982). Spatial invariance of receptive field location in the presence of eye movements of fixation for neurons in monkey striate cortex. *Society for Neuroscience Abstracts,* 8, 707.
Motter, B.C. and Poggio, G.F. (1990) Dynamic stabliziation of receptive field sof cortical neurons (VI) during fixation of gaze in the macaque. *Exp. Brain Res.* 83, 37-43.
Mullen, K.T. (1985) The contrast sensitivity of human colour vision to red-green and blue-yellow chromatic gratings. *J. Physiol. (Lond.)* 359, 381-409.
Nealey, T.A., Ferrara,, V.P., & Maunsell, J.H.R. (1991) Magnocellular and parvocellular contributions to the ventral extrastriate cortical processing stream. *Soc. Neurosci. Abstr.* 17:525.
Noorlander, C., & Koenderink, J. J. (1983). Sensitivity to spatial-temporal color contrast in the periphery visual field. *Vision Research,* 23, 1-11.
Ogren, M. P., & Hendrickson, A. E. (1977). The distribution of pulvinar terminals in visual areas 17 and 18 of the monkey. *Brain Research,* 137, 343-350.
Olshausen, B.A., Anderson, C.H., and Van Essen, D.C. (1993) A neurobiological model of visual attention and invariant pattern recognition based on dynamic routing of information. J. Neurosci., 14: 4700-4719.
O'Kusky, J., & Colonnier, M. (1982). A laminar analysis of the number of neurons, glia, and synapses in the visual cortex (area 17) of adult macaque monkeys. *Journal of Comparative Neurology,* 210, 178-290.
Østerberg, G. (1935). Topography of the layer of rods and cones in the human retina. *Acta Ophthalmologica,* 65, 1-102.
Peichl, L., & Wässle, H. (1979). Size, scatter and coverage of ganglion cell receptive field centres in the cat retina. *Journal of Physiology,* 291, 11 7- 141.
Perrett, D. I., Mistlin, A. J., & Chitty, A. J. (1987). Visual neurones responsive to faces. *Trends in NeuroSciences, 10,* 358-364.
Perry, V. H., & Cowey, A. (1985). The ganglion cell and cone distributions in the monkey's retina: Implications for central magnification factors. *Vision Research,* 12, 1795-1810
Perry, V. H., Oehler, R., & Cowey, A. (1984). Retinal ganglion cells that project to the dorsal lateral geniculate nucleus in the macaque monkey. *Neuroscience,* 12, 1101 - 1123.
Peterhans, E. and von der Heydt, R. (1993) Functional organization of area V2 in the alert macaque. Eur. J. Neurosci. 5:509-524.
Poggio, G. F. (1984). Processing of stereoscopic information in primate visual cortex. In G. Edelman, W. E. Gall, & W. M. Cowan (Eds.), *Dynamic aspects of neocortical function.* New York: Wiley.
Pollen, D. A., Gosh, J. P., & Jacobsen, L. D. (1988). Responses of simple and complex cells to compound sine-wave gratings. *Vision Research,* 28, 25-39.
Posner M. I., & Presti, D. E. (1987). Selective attention and cognitive control. *Trends in NeuroSciences, 10,* 13-17.
Purpura, K., Kaplan, E., & Shapley, R. M. (1988). Background light and the contrast gain of primate P and retinal ganglion cells. P*oceedings of the National Academy of Sciences of the United States of America,* 8S, 4534-4537.
Reid, R.C. & Shapley, R.M. (1992) Spatial structure of cone inputs to receptive fields in primate lateral geniculate nucleus. *Nature* 356, 716-718.
Rockland, K. S., & Pandya, D. N. (1979). Laminar origins and termination of cortical connections of the occipital lobe in the rhesus monkey. *Brain Research, 179,* 3-20.
Rodieck, R. W. (1988). The primate retina. In *Comparative primate biology. (Vol.* 4). New York: Liss.
Rolls, E. T., & Baylis, G. C. (1986). Size and contrast have only small effects on the responses to faces of neurons in the cortex in the superior temporal sulcus. *Experimental Brain Research,* 65, 38-48.
Rovamo, J., & Virsu, V. (1979). An estimation and application of the human cortical magnification factor. *Experimental Brain Research,* 37, 495-510.

Schein, S.J. (1988). Anatomy of macaque fovea and spatial densities of neurons in foveal representation. *Journal of Comparative Neurology,* 269, 479-505.

Schein, S. J., & De Monasterio, F. M. (1987). Mapping of retinal and geniculate neurons onto striate cortex of macaque. *Journal of Neuroscience, 7,* 996-1009.

Schneider, W. (1985). Toward a model of attention and the development of automatic processing. In M. l. Posner & O. S. M. Marin (Eds.), *Attention and performance (Vol. Xl).* Hillsdale, NJ: Erlbaum.

Schwartz, E. L. (1980). Computational anatomy and functional architecture of striate cortex: A spatial mapping approach to perceptual coding. *Vision Research,* 20, 645~69.

Shapley, R., & Perry, V. H. (1986). Cat and monkey retinal ganglion cells and their visual functional roles. *Trends in NeuroSciences* 9, 229.

Sherman, S. M., & Koch, C. (1986). The control of retinogeniculate transmission in the mammalian lateral geniculate nucleus. *Experimental Brain Research,* 63, 1-20

Silveira, L.C.L.& Perry, V.H. (1991) The topography of magnocellular projecting ganglion cells (m-ganglion cells) in the primate retina. *Neuroscience* 40, 217-237.

Snyder, A. W., & Miller, W. H. (1977). Photoreceptor diameter and spacing for highest resolving power. *Journal of the Optical Society of America,* 67, 696-698.

Somogyi, P., Freund, T. F., & Cowey, A. (1982). *The* axo-axonic interneuron in the cerebral cortex of the rat, cat and monkey. *Neuroscience,* 7, 2577-2607.

Toet, A., van Eekhout, M. P., Simons, H. L. J. J., & Koenderink, J. J. (1987). Scale invariant features of differential spatial displacement discrimination. *Vision Research,* 27, 441-451.

Tootell, R. B. H., Silverman, M. S., Hamilton, S. L., Switkes, E., & DeValois, R. L. (1988). Functional anatomy of macaque striate cortex. V. Spatial frequency. *Journal of Neuroscience,* 8, 1610-1624.

Tootell, R. B. H., Switkes, E., Silverman, M. S. & Hamilton, S. L. (1988). Functional anatomy of macaque striate cortex. II. Retinotopic organization. *Journal of Neuroscience*, 8, 1531-1568.

Ts 'o, D. Y., & Gilbert, C. D. (1988). *The* organization of chromatic and spatial interactions in the primate striate cortex *Journal of Neuroscience,* 8, 1712-1727.

Ungerleider, L. G., & Mishkin, M. (1982). Two cortical visual systems. In D. J. Ingle, M. A. Goodale, & R. J. W. Mansfield (Eds.), *Analysis of visual behavior*. Cambridge, MA: MIT Press.

van Doorn, A. J., Koenderink, J. J., & Bouman, M. A. (1972). The influence of the retinal inhomogeneity on the perception of spatial patterns. *Kybernetic,* 10, 223-230.

Van Essen, D. C., & Anderson, C. H. (1986). Sampling of the visual image in the retinal and LGN of the macaque: A quantitative model. *Investigative Ophthalmology & Visual Science Suppl.,* 27, 94.

Van Essen, D.C. & Anderson, C.H. (1990) Reference frames and dynamic remapping processes in vision. In: *Computational Neuroscience*, (Ed.) E. Schwartz, MIT Press, Cambridge, MA, pp. 278-294.

Van Essen, D.C. Anderson, C.H., & Felleman, D.J. (1992) Information processing in the primate visual system: an integrated systems perspective. *Science*.255, 419-423.

Van Essen, D.C. & DeYoe, E.A. (1993) Concurrent processing in the primate visual cortex. In: *The Cognitive Neurosciences*,, M.S. Gazzaniga, ed, MIT Press, Cambridge, MA, pp. 383-400.

Van Essen D. C., DeYoe, E. A., Olavarria, J. F., Knierim, J. J., Sagi, D. Fox, J. M., & Julesz, B. (1989). Neural responses to static and moving texture patterns in visual cortex of the macaque monkey. In D. M. V, Lam & C. Gilbert (Eds.), *Neural mechanisms of visual perception*. Woodlands, TX: Portfolio Publishing, pp. 135-153.

Van Essen, D. C., & Maunsell, J. H. R. (1983). Hierarchical organization and functional streams in the visual cortex *Trends in NeuroSciences,* 6, 370-375.

Van Essen, D. C., Newsome, W. T., & Maunsell, J. H. R. (1984). The visual field representation in striate cortex of the macaque monkey: Asymmetries, anisotropies, and individual variability *Vision Research, 24,* 429-448.

Van Essen, D.C., Olshausen, B., Anderson, C.H. & Gallant, J.L. (1991) Pattern recognition, attention, and information bottlenecks in the primate visual system. In: *Proc. SPIE Conf. on Visual Information Processing: From Neurons to Chips*, vol. 1473, 17-28. -

Van Essen, D.C., Olshausen, B., Gallant, J., Press, W., Anderson, C., Drury, H., Carman, G. & Felleman, D. (1993) Anatomical, physiological, and computational aspects of hierarchical processing in the macaque visual cortex. In: Structural and Functional Organization of the Neocortex, C. Nothdurft, ed., in press.

Virsu, V., & Rovamo, J. (1979). Visual resolution, contrast sensitiv ity, and the cortical magnification factor. *Experimental Brain Research,* 37, 475-494.

Wässle, H., Grunert, U., Rohrenbeck, J. and Boycott, B. (1990). Retinal ganglion cell density and cortical magnification factor in the primate retina. Vision Res. 30, 1897-1911.

Wässle, H. and Boycott, B. B. (1991). Functional architecture of the mammalian retina. Physiological Reviews 71, 447-480.

Watanabe, M. & Rodieck, R.W. (1988) Parasol and midget ganglion cells of the primate retina. *J. Comp. Neurol.* 289:434-454.

Wehmeier, U.. Dong, D., Koch, C., & Van Essen, D. C. (1989 Modeling the mammalian visual system. In C. Koch & 1. Segev (Eds.), *Methods in neuronal modeling: From synapses to net works*. Cambridge, MA: MIT Press.

Westheimer, G. (1979). Scaling of visual acuity measurement *Archives of Ophthalmology* 97, 327-330.

Williams, D. R. (1988). Topography of the foveal cone mosaic in. the living human eye. *Vision Research,* 28,433-454.

Williams, D. R., & Collier, R. (1983). Consequences of spatial sampling by a human photoreceptor mosaic. *Science,* 221 385-387.

Wilson, M. A., & Bower, J. M. (1989). The simulation of large-scale neural networks. In C. Koch & 1. Segev (Eds.) *Methods in neuronal modeling: From synapses to network.* Cambridge, MA: MIT Press.

Wise, S. P., & Desimone, R. (1988). Behavioral neruophysiology: Insights into seeing and grasping. *Science,* 242, 736-741.

Wolbarsht, M. L., Wagner, H. G., & Ringo, J. L. (1985). Retinal, mechanisms for improving visual acuity. In A. Fein & J. Sj Levine (Eds.), *The visual system*. New York: Liss.

Zeki, S. M. (1978). Functional specialisation in the visual cortex of the rhesus monkey. *Nature,* 274,423.

Zeki, S., & Shipp, S. (1988). The functional logic of cortical connections. *Nature,* 335, 311-317.